*Manuscript
Click here to view linked References

Regulation of Ahr signaling by Nrf2 during development: Effects of Nrf2a deficiency on PCB126 embryotoxicity in zebrafish (*Danio rerio*)

Michelle E. Rousseau[1], Karilyn E. Sant[1], Linnea R. Borden[1], Diana G. Franks[2], Mark E. Hahn[2], Alicia R. Timme-Laragy[1,2,*]

1. Department of Environmental Health Sciences, School of Public Health and Health Sciences, University of Massachusetts Amherst, Amherst, MA 01003
2. Biology Department, Woods Hole Oceanographic Institution, Woods Hole, MA 02543

* Corresponding author, 686 N. Pleasant St., Goessmann 149C, Amherst, MA 01003, phone 413-545-7423

Michelle E. Rousseau merousse@umass.edu

Karilyn E. Sant ksant@umass.edu

Linnea R. Borden lborden@umass.edu

Diana G. Franks dfranks@whoi.edu

Mark E. Hahn mhahn@whoi.edu

Alicia R. Timme-Laragy aliciat@umass.edu

Abstract

The embryotoxicity of co-planar PCBs is regulated by the aryl hydrocarbon receptor (Ahr), and has been reported to involve oxidative stress. Ahr participates in crosstalk with another transcription factor, Nfe2l2, or Nrf2. Nrf2 binds to antioxidant response elements to regulate the adaptive response to oxidative stress. To explore aspects of the crosstalk between Nrf2 and Ahr and its impact on development, we used zebrafish (*Danio rerio*) with a mutated DNA binding domain in Nrf2a (*nrf2a*$^{fh318/fh318}$), rendering these embryos more sensitive to oxidative stress. Embryos were exposed to 2 nM or 5 nM PCB126 at 24 hours post fertilization (prim-5 stage of pharyngula) and examined for gene expression and morphology at 4 days post fertilization (dpf; protruding –mouth stage). Nrf2a mutant eleutheroembryos were more sensitive to PCB126 toxicity at 4 dpf, and in the absence of treatment also displayed some subtle developmental differences from wildtype embryos, including delayed inflation of the swim bladder and smaller yolk sacs. We used qPCR to measure changes in expression of the *nrf* gene family, *keap1a, keap1b,* the *ahr* gene family, and known target genes. *cyp1a* induction by PCB126 was enhanced in the Nrf2a mutants (156-fold in wildtypes vs. 228-fold in mutants exposed to 5 nM). Decreased expression of heme oxygenase (decycling) 1 (*hmox1*) in the Nrf2a mutants was accompanied by increased *nrf2b* expression. Target genes of Nrf2a and AhR2*,* NAD(P)H:quinone oxidoreductase 1 (*nqo1*) and glutathione S-transferase, alpha-like (*gsta1*), showed a 2-5-fold increase in expression in the Nrf2a mutants as compared to wildtype. This study elucidates the interaction between two important transcription factor pathways in the developmental toxicity of co-planar PCBs.

Key Words: transcription factor, dioxin-like compound, gene expression, embryonic development, swim bladder, yolk

Abbreviations:

Ahr: aryl hydrocarbon receptor
Ahrr: aryl hydrocarbon receptor repressor
ARE: antioxidant response element
Cyp1a: cytochrome P540 1a
DLC: dioxin-like compound
DMSO: dimethyl sulfoxide
dpf: days post fertilization
hpf: hours post fertilization
Keap1: Kelch-like ECH-associated protein 1
Nrf2: nuclear factor erythroid related factor 2-like-2
PAH: polycyclic aromatic hydrocarbon
PCB126: 3,3',4,4',5-pentachlorobiphenyl
ROS: reactive oxygen species
tBOOH: *tert* butylhydroperoxide
tBHQ: *tert* butylhydroquinone
TCDD: 2,3,7,8-tetracholordibenzo-p-dioxin
XRE: xenobiotic response element, aka dioxin response element

1. **Introduction**

PCBs are carcinogenic and teratogenic persistent organic pollutants. Along with other dioxin-like-compounds, co-planar PCBs are potent, chlorinated ligands for the aryl hydrocarbon receptor (Ahr), which has been shown to mediate toxicity in numerous mammalian and fish species (e.g. rev. in (Bock, 2013; Denison *et al.*, 2011; Hahn *et al.*, 2006; King-Heiden *et al.*, 2012)). These ligands for the Ahr are also associated with oxidative stress, such as via uncoupling of the cytochrome P450 catalytic cycle and the release of superoxide and/or hydrogen peroxide (Dalton *et al.*, 2002). The adaptive response to oxidative stress is largely regulated by the redox-sensitive transcription factor nuclear factor erythroid related factor 2-like-2 (Nfe2l2 or Nrf2- see footnote). Nrf2 regulates transcription of numerous antioxidant and cytoprotective genes, and also participates in crosstalk with the Ahr to regulate transcription of genes, many of which encode Phase I and Phase II enzymes (Wakabayashi *et al.*, 2010).

The Ahr is a member of the basic helix-loop-helix Per-Arnt-Sim (bHLH/PAS) family of transcription factors. Briefly, it is a constitutively expressed, cytosolic protein. In the canonical Ahr activation pathway, Ahr translocates to the nucleus upon ligand binding, where it forms a heterodimer with the aryl hydrocarbon nuclear translocator (Arnt). This heterodimer binds to the xenobiotic response element (XRE) in promoter regions and initiates the transcription of a variety of genes. These genes are mostly comprised of Phase I and Phase II enzymes which are often referred to as the "classical Ahr gene battery," but also include target genes involved in numerous other functions including liver development, cell cycle progression, cellular differentiation, inflammation, and cancer (Bock, 2013; Denison, et al., 2011).

Zebrafish have three Ahr genes (*ahr1a, ahr1b, ahr2*), whereas most mammals have only one (*Ahr*). Ahr2 has been shown to mediate the effects of 3,3',4,4',5-pentachlorobiphenyl (PCB126), 2,3,7,8-tetracholordibenzo-p-dioxin (TCDD; dioxin), and some high molecular-weight PAHs; the roles of Ahr1a and Ahr1b are not yet fully understood (Andreasen *et al.*, 2002; Garner *et al.*, 2013; Goodale *et al.*, 2012; Jonsson *et al.*, 2007; Karchner *et al.*, 2005; Prasch *et al.*, 2003). PCB126 exposure in zebrafish embryos has been shown to induce expression of *cyp1a*, *cyp1b1*, *cyp1c1*, and *cyp1c2* in an Ahr2-mediated manner (Billiard *et al.*, 2006; Jonsson, et al., 2007). *cyp1a* has been shown to be the most responsive of the *cyp1* genes, and either expression of this gene or enzyme activity (ethoxyresorufin O-deethylase; EROD) is often used as a biomarker of Ahr ligand activation. Numerous studies of zebrafish embryos exposed to PCB126 or TCDD during development have demonstrated a suite of morphological deformities collectively referred to as "blue sac disease," which includes pericardial edema, craniofacial and

heart malformations, and reduced swim bladder inflation; these deformities have been shown to be primarily regulated by Ahr2 (Garner, et al., 2013; Jonsson, et al., 2007; Jonsson *et al.*, 2012; Lanham *et al.*, 2014; Prasch, et al., 2003), although the importance of other signaling pathways has also been demonstrated, including interactions with Wnt, Cox-2, Sox9 (Yoshioka *et al.*, 2011).

In addition to activating Ahr2, exposure to co-planar PCBs and dioxins has also resulted in the generation of reactive oxygen species (ROS) and/or oxidative stress in mammals, frogs, birds, and fish, via several mechanisms including generation of reactive metabolites, an increase in mitochondrial respiration and hydrogen peroxide, uncoupling of the cytochrome P450 catalytic cycle, glutathione depletion, and inflammation (Dalton, et al., 2002; Gillardin *et al.*, 2009; Lu *et al.*, 2011; Nebert *et al.*, 2000; Schlezinger *et al.*, 2000; Schlezinger *et al.*, 2006; Senft *et al.*, 2002). Oxidative stress is defined as a loss of redox signaling and control (Jones, 2006), and the oxidative stress response is defined as the resulting changes in gene expression that serve to mitigate the oxidative challenge (Hahn *et al.*, 2014). Despite the many studies that demonstrate an oxidative stress response to these co-planar PCBs and dioxins, there have also been studies that have failed to identify an oxidative stress response. In zebrafish for example, while *nrf2a* has been shown to be up-regulated by TCDD (Hahn, et al., 2014), zebrafish embryos sampled immediately after a 6 h exposure to TCDD showed no evidence of altered expression of other genes typically found in the oxidative stress response at 4 dpf, and there was an increase in *gstp1* expression only after 48 h of a TCDD exposure that began at 24 hours post fertilization (hpf) (Hahn, et al., 2014). An oxidative stress response was not observed in response to TCDD at least two other studies (Alexeyenko *et al.*, 2010; Wang *et al.*, 2013). This may be due to many factors including differences in timing, dose, developmental stage, species sensitivity to Ahr ligand binding, or exposure duration, or it is possible that ROS generation may not always be sufficient to alter redox signaling or activate an oxidative stress response.

Nrf2 has been designated the “master regulator” of the adaptive response to oxidative stress (Ohtsuji *et al.*, 2008). Nrf2 is a basic-region leucine zipper transcription factor that is constitutively and ubiquitously expressed and bound to Kelch-like ECH-associated protein 1 (Keap1) within the cytosol, targeting it for ubiquitination (Cullinan *et al.*, 2004). There are several ways in which Nrf2 can be activated, such as protein kinase RNA-like endoplasmic reticulum kinase (PERK) signaling from the endoplasmic reticulum, phosphorylation, and electrophilic or ROS interactions (reviewed in (Bryan *et al.*, 2013; Niture *et al.*, 2014)). After activation, Nrf2

accumulates in the nucleus where it dimerizes with small v-maf avian musculoaponeurotic fibrosarcoma oncogene homolog (Maf) proteins to upregulate transcription of numerous cytoprotective genes (Ma *et al.*, 2004). Nrf2 mediates gene expression through the antioxidant response element (ARE). AREs are frequently located in promoter regions of genes involved in the oxidative stress response and Phase II detoxification, but also have more pleiotropic roles in functions such as cell cycle regulation and lipid metabolism (Malhotra *et al.*, 2010). Disruption of NRF2 in mice has been linked to an increase in pulmonary inflammation, emphysema, neurodegeneration, and chemical carcinogenesis, thus indicating the importance of Nrf2's cytoprotective role (Kensler *et al.*, 2007). NRF2 knockout mice have also been shown to have defects in liver growth and size (Beyer *et al.*, 2008), reduced bile duct microbranching (Skoko *et al.*, 2014), and retinal vasculature density (Wei *et al.*, 2013); in some genetic backgrounds, NRF2-/- mice have a congenital defect resulting in an intrahepatic shunt (Skoko, et al., 2014).

Zebrafish have partitioned the function of Nrf2 between two genes, *nrf2a* and *nrf2b* (reviewed in (Hahn *et al.*, 2015)). We have previously shown that Nrf2a is generally involved in activating gene expression, while Nrf2b is involved in repressing gene expression (Timme-Laragy *et al.*, 2012). The *nrf2a*^{fh318} mutant is a recessive loss-of-function allele generated via the zebrafish Targeted Induced Local Lesions in Genomes (TILLING) mutagenesis project (Mukaigasa *et al.*, 2012). The phenotype of *nrf2a*^{fh318} fish is similar to that of NRF2 -/- mice (e.g (Itoh *et al.*, 1997)) in that they display normal development and reproduction and enhanced sensitivity to oxidants (Mukaigasa, et al., 2012). *nrf2a*^{fh318} larvae are more sensitive to oxidative stress, but no morphologic or growth differences between Nrf2a mutant vs. wildtype larvae or adults have been identified (Mukaigasa, et al., 2012).

Crosstalk between Ahr and Nrf2 has been demonstrated in mammalian systems and has been shown to be important in the transcriptional regulation of genes encoding many Phase I and Phase II detoxification enzymes (Anwar-Mohamed *et al.*, 2011; Lo and Matthews, 2013; Miao *et al.*, 2005; Tijet *et al.*, 2006; Wang, et al., 2013; Yeager *et al.*, 2009). TCDD has been shown to increase both protein level and nuclear accumulation of NRF2 in mice (Yeager, et al., 2009) and in Hepa1c1c7 cells (Wang, et al., 2013), without evidence of oxidative stress; rather, Wang et al. provided evidence suggesting the AHR upregulated transcription of NRF2 and formed protein complexes with both NRF2 and KEAP1 that contributed to the stability of NRF2 and subsequent ARE-activation (Wang, et al., 2013). However, the interactions of these pathways have not been thoroughly studied during embryonic development, which is a critical time for chemical sensitivity that is fundamentally different than adult physiology.

Zebrafish contain multiple paralogs of both Ahr and Nrf2, each of which demonstrates a seemingly different function. Here, we tested the hypothesis that Nrf2a plays a protective role in PCB126 embryotoxicity. We used PCB126 as a model ligand to study the interaction between the Ahr and Nrf2 pathways during embryonic development in zebrafish embryos lacking a functional Nrf2a. We present data on differential sensitivity to PCB126 embryotoxicity between the Nrf2a mutant and wildtype eleutheroembryos, differential gene expression of *ahr* and *nrf*-family members and target genes, and also identify subtle developmental differences between the two genotypes.

2. Materials and Methods

2.1 Chemicals

Polychlorinated biphenyl-126 (PCB126) was purchased from Ultra Scientific (N. Kingstown, RI, USA), and was dissolved in dimethyl sulfoxide (DMSO, Fisher Scientific, Pittsburgh, PA, USA). Solutions were vortexed prior to use. *Tert*-butylhydroquinone (tBHQ) was purchased from Acros Organics (Thermo Fisher Scientific, Waltham, MA, USA).

2.2 Animals

Zebrafish heterozygous for the *nrf2a*^{fh318} and *nrf2a*^{fh319} alleles were generated through the TILLING mutagenesis Project (R01HD076585) and obtained as embryos from the Moens Laboratory (Fred Hutchinson Cancer Research Center, Seattle, WA, USA). This project aims to generate loss-of-function mutations in zebrafish genes. The *nrf2a*^{fh318} and *nrf2a*^{fh319} alleles encode Nrf2a proteins with point mutations resulting in single amino acid changes. Both of these mutations are located within the DNA binding domain that associates with AREs, and the wild type residue at these locations is conserved between zebrafish Nrf2a, human, mouse, and the chicken orthologs. The fh318 allele point mutation results in a change from R to L at amino acid 479 and the fh319 allele results in a change from N to I at amino acid 488; these amino acid residue numbers are derived from the TILLING project background sequence. Because these changes are in the DNA-binding domain, *nrf2a* should still be transcribed and translated, and still maintain a functional relationship with Keap1a and Keap1b (the zebrafish co-orthologs of the mammalian Keap1 (Li *et al.*, 2008)). When we amplified, cloned, and sequenced the full-length *nrf2a*^{fh318} and *nrf2a*^{fh319} cDNAs (see below), we found a discrepancy between the TILLING *nrf2a* sequence and our sequences, with the TILLING sequence missing a six amino acid segment between residues 186-193. Supplemental Figure 1 shows the protein alignment encoded by the *nrf2a*-318-2 clone with other zebrafish Nrf2a sequences including the TILLING

sequence. Our sequence agrees with that identified by (Mukaigasa, et al., 2012), which numbers the changed amino acids as R485L and N494I for the *nrf2a*^{fh318} and *nrf2a*^{fh319} alleles, respectively.

Adult fish were maintained at 28.5°C on a 14 hour (h) light cycle, 10 h dark light cycle in an Aquatic Habitats zebrafish system (for experiments conducted at the Woods Hole Oceanographic Institution (WHOI)) or an Aquaneering zebrafish system (at the University of Massachusetts Amherst (UMASS)). To obtain homozygous wildtype and mutant fish, the heterozygous adults were crossed against Tubigen-longfin (TL) wildtype fish for two generations, then in-crossed and genotyped. Adult homozygous zebrafish were crossed to obtain homozygous wildtype (*nrf2a* $^{+/+}$) or mutant (*nrf2a* $^{fh318/fh318}$) embryos. All embryos were maintained at low density with daily water changes at 28.5°C on a 14 h light cycle, 10 h dark light cycle in 0.3x Danieau's water throughout the duration of the experiment. This study was conducted in accordance with the recommendations in the Guide for the Care and Use of Laboratory Animals of the National Institutes of Health. Animal protocols were approved by the Institutional Animal Care and Use Committees (IACUCs) of WHOI (Woods Hole, MA, USA, Animal Welfare Assurance Number A3630-01) and UMASS (Amherst, MA, USA, Animal Welfare Assurance Number A3551-01).

2.3 Genotyping

To identify mutant (*nrf2a*^{fh318}) and wildtype alleles (*nrf2a*$^{+}$), we isolated DNA from individual fish fin clips using standard methods. Briefly, the fin was digested with proteinase K overnight, then subjected to a phenol-chloroform DNA extraction. DNA was quantified using a BioDrop µLITE (BioDrop, Cambridge, UK), and only samples that met quality control standards (260/280 ratio 1.8-2) were used in subsequent steps. For the PCR reaction, 200 ng of DNA was amplified using a proofreading polymerase (Advantage polymerase, Clontech, Mountain View, CA, USA), in a 25 µL reaction containing 10 mM dNTPs, 10 µM Reverse primer (5' - ACC AAC AGG CGG CGA TAA TGA CTT – 3'), and 10 µM forward primer (5'- AAC GAT GGC TCC CAG ACT CCA CT – 3'). The PCR reaction was carried out on an Eppendorf Mastercycler Nexus Gradient thermocycler (Eppendorf, Hauppauge, NY, USA). The PCR conditions were 94°C for 10 min, then 35 cycles of 94°C for 10 seconds, 62.9°C for 30 seconds, and 72°C for 60 seconds. This was followed by a 7 minute incubation at 72°C, then the reaction was cooled and held at 4°C. This resulted in one clear band of 835 bp. This product was then cut with the restriction enzyme Hpy99I and Cut Smart Buffer (New England Biolabs, Ipswich, MA, USA) in a 25 µL reaction containing 1 µL of PCR product for two h at 37°C. The fh318 mutation in the *nrf2a* gene results

in an amino acid change from an R to an L at amino acid 485. The restriction enzyme cut the wildtype sequence resulting in two bands, at 530 and 305 bp, while the mutant sequence remained uncut. To visualize the bands, 10 µL of the reaction was mixed with 4 µL of MaestroSafe loading buffer (MaestroGen, Las Vegas, NV, USA), run on a 2% agarose electrophoresis gel, and imaged on a Syngene Pxi (Syngene, Frederick, MD, USA).

2.4 Cloning of Nrf2a alleles

To assess the functional consequences of the *nrf2a* point mutations *in vitro*, we amplified the full-length *nrf2a*^{fh318} and *nrf2a*^{fh319} cDNAs, cloned them into pcDNA and verified the sequences. To clone these mutant genes, total RNA was isolated from the fin of one *nrf2a*^{fh318} mutant fish and 20-pooled embryos collected from *nrf2a*^{fh319} mutant fish using STAT-60 (Tel-Test, Inc., Friendswood, TX, USA). Total RNA isolated from embryos collected from *nrf2a*^{fh319} fish containing the wild-type allele (as determined through fin-clipping and genotyping) was used as the negative control. Total RNA was quantified by Nanodrop (Thermo Fisher Scientific), and cDNA synthesized using the iScript kit (Biorad, Hercules, CA, USA) from 1 µg of total RNA. PCR was run to amplify the full-length *nrf2a* gene using primers that incorporated XbaI and HindIII restriction enzyme sites at the 5' end of each primer, facilitating ligation into the pcDNA 3.2/DEST vector. Using Advantage II Polymerase (Clontech), the PCR program was as follows: 94°C, 1 minute; 5 cycles of 94°C, 30 seconds, 60°C, 15 seconds, 68°C, 2 minutes; 30 cycles of 94°C, 5 seconds, 68°C, 2 minutes. PCR products were run on a 1% agarose gel, and the product bands extracted and gene-cleaned (MP Biomedicals, Santa Ana, CA, USA). The gene-cleaned PCR products, along with 1 µg pcDNA plasmid DNA, were cut with HindIII/XbaI (Promega, Madison, WI) for 2 h at 37°C. The cut products were again gene-cleaned to remove the restriction enzymes, and the *nrf2a*^{fh318}, *nrf2a*^{fh319}, and *nrf2a*$^{+}$ non-mutant allele derived from the fh319 heterozygous line were ligated onto linear pcDNA. These ligations were transformed into JM109 competent cells with resulting transformants spread on LB plates supplemented with ampicillin and incubated overnight at 37°C. Single colonies were picked into 2 ml LB ampicillin liquid cultures and grown overnight at 37°C with shaking. Plasmid mini-preps were made using the Pure Yield Plasmid kit (Promega). To screen for mutants, plasmid DNA from the *nrf2a*^{fh318} clones was cut with restriction enzyme Hpy99I as described above. Plasmid DNA from the nrf2a^{fh319} clones was cut with BglII for 2 h at 37°C. Cut products were run on a 1% agarose gel, and clones positive for the insert were sent to Eurofins-MWG (Birmingham, AL, USA) for sequencing. Large plasmid preps (Qiagen, Valencia, CA, USA) were made from the *nrf2a*-318-2

mutant clone, and the *nrf2a*-319S mutant clone. These preps were used in the luciferase assay described below.

2.5 Transient transfection of mutant and wildtype alleles and luciferase assay

Three 48-well cell culture plates were seeded with Cos-7 cells (African Green Monkey Kidney, from ATCC, Manassas, VA, USA) at a density of 1.6 x10^5 cells/ml, and 250 µl/well. Plates #1 and #2 were identical, and used for transfection, while plate #3 cells were used to check the expression level of the Nrf2a proteins, by western blot with antibodies against Nrf2a. Cos-7 cells in the plates were grown at 37°C with 5% CO_2 for 24 h prior to transfection. X-tremeGENE HP DNA transfection reagent (Roche, Genentech, S. San Francisco, CA, USA) was used at a 3:1 ratio of reagent: DNA. Transfection components and their concentrations were as follows: 50 ng/well ARE-luciferase, 3 ng/well Renilla, 25 ng/well wild type *nrf2a* DNA (pCS2-*nrf2a*, a generous gift from Dr. Makoto Kobyashi, University of Tsukuba, Tennodai, Tsukuba, Japan (Kobayashi *et al.*, 2002)), 25 ng/well *nrf2a*-318-2 mutant DNA, 25 ng/well *nrf2a*-319-S mutant DNA, 50 ng/well zf-*keap-1a* DNA, and 50 ng/well zf-*keap-1b* DNA (both *keap1* plasmids were also a gift from Dr. Kobayashi). Plate #1 cells were dosed with DMSO, while cells in plate #2 were dosed with 10 µM tBHQ at 19 hours post transfection for 5 h. The luciferase assay was run using the Dual-Luciferase Reporter Assay System (Promega), and fluorescence was read on a Turner TD 20/20 Luminometer. Wells on the Western Blot plate were transfected with 50 ng or 500 ng nrf2a, nrf2a-318-2, or nrf2a-319S DNA only. After 15 h, the cells were rinsed with 1x PBS, and collected in 40 µl 2x sample treatment buffer/well. Six replicate wells of cell lysates were pooled into a 1.5 ml Eppendorf tube, boiled for 5 minutes and frozen at -80°C.

Cell lysates were loaded on an 8% acrylamide gel, 30 µl of lysate/well, and run at 100V for 2 h. The proteins were transferred to a Nytran substrate using the semi-dry transfer method, and blocked in milk/TBST solution overnight at 4°C. The primary antibody used was Nrf2a rabbit #5136 antibody at 1 µg/ml, with goat-anti-rabbit horse-radish peroxidase (GARHRP) secondary antibody at 1:5000. Blots were exposed to the enhanced chemiluminescence (ECL) Prime Western Blotting Detection Reagent (Amersham, GE Healthcare Biosciences, Piscataway, NJ, USA), and images developed on Hyperfilm ECL (Amersham). The Nrf2a antibody was generated by 21st Century Biochemicals (Marlboro, MA, USA) against the Nrf2a-specific peptide sequence NMPMQETLDMNAFMKPST, and validated using standard procedures.

2.6 PCB Exposure

The model Ahr ligand used in this study was PCB126. At 24 hpf (prim-5 of the pharyngula stage, hereforth referred to as 24 hpf as per staging by (Kimmel *et al.*, 1995)), embryos were exposed for 24 h in triplicate pools of 5 embryos per dose, in 20 mL glass vials. DMSO concentration was 0.01 % in both control and PCB-treated embryo groups, in a total volume of 10 mL 0.3x Danieau's water. The concentrations of PCB126 included 2 nM and 5 nM. At 4 dpf (protruding mouth stage, hereforth referred to as 4 dpf), embryos were either imaged for morphology, or fixed in 100 µL of RNA later (Ambion, Life Technologies, Grand Island, NY, USA) and stored at -80°C until RNA extraction. Morphology experiments were repeated three times; two of these were analyzed at 4 dpf, and a third at 5 dpf.

2.7 Morphometrics

At 4 dpf, eleutheroembryos were mounted in 3% methylcellulose and imaged on a Zeiss dissecting microscope with a Zeiss AxioCam MR Color CCD camera at 50x magnification (Zeiss, Peabody, MA, USA). Zeiss Axiocam software was used to take measurements of the pericardial area, an assessment made as to whether the swim bladder was inflated, and a deformity score assessing the truncation of Meckel's cartilage was given using previously established parameters that incorporate both frequency and severity (Harbeitner *et al.*, 2013). The ventral-dorsal distance was measured by dropping a straight line from the third somite to the bottom of the yolk sac.

To measure the yolk area of early stage embryos, 19 *nrf2a*$^{+/+}$and 20 *nrf2a*$^{fh318/fh318}$ blastula-stage embryos (3 hpf), embryos were imaged on an EVOS Auto FL at 100x magnification. To standardize measurement of yolk sacs, the diameter was measured twice. The first measurement began at the edge of the yolk sac closest to the center of the embryonic cell mass, and this line extended to the furthest point across the yolk sac. The second diameter measurement was of the line perpendicular to the first one. The volume for an ellipse was used to calculate yolk sac area: $A = \pi ab$, where "a" is the radius of one measurement, and "b" is the radius of the other (0.5*diameter). Results are reported in microns^2 (μm^2).

2.8 Total RNA extraction and reverse transcription

RNA extractions were carried out according to the GeneJET RNA Purification Kit Total RNA Purification Protocol (Thermo Fisher Scientific Inc,, Waltham, MA, USA). RNA quality and quantity was analyzed spectrophotometrically using a BioDrop µLITE (BioDrop, Cambridge, UK, USA). The iScript cDNA Synthesis Kit for reverse transcription PCR (Bio-Rad Laboratories,

Hercules, CA, USA) was used according to the manufacturer's instructions using 360 ng of RNA and carried out in an Eppendorf Mastercycler Nexus Gradient thermocycler (Eppendorf, Hauppauge, NY, USA) according the reaction protocol provided by iScript.

2.9 Quantitative real-time PCR

cDNA was diluted to a working concentration of 0.125 ng/µL. A 20 µL qPCR reaction contained 5 pM of each primer, 10 µL 2x iQ SYBR Green Supermix (Bio-Rad), 5 µL nuclease free water and 0.5 ng cDNA template (4 µL of 0.125 ng/µL). qRT-PCR was performed in a Bio-Rad CFX Connect Real-Time System under the following thermal cycle conditions: 3 min at 95^{o}C, followed by 40 replicates of 15 s at 95^{o}C, then 60 – 68^{o}C depending on the melt temperature of the primers used for each gene (see **Supplemental Table 1**). A dissociative curve calculation step was completed one time at the end of each. All primers have been previously validated for efficiency and specificity. All samples were run in technical duplicates and each run included a no-template control.

qPCR data were analyzed using the Bio-Rad CFX Manager Software, Version 3.0 (Bio-Rad). The $\Delta\Delta C_T$ method was used to calculate fold change compared to ***β-actin***. Values are presented as mean ± SEM, and *N* is defined as the number of pools of embryos. Expression of the reference genes (***β-actin*** and *elongation factor 1-alpha (ef1a)*) was not altered by any of the treatments.

2.10 Bioinformatics

Genes that were measured by qPCR were also searched for putative AREs in the region from 10 kb upstream of the transcriptional start site through the end of the 2nd exon. Zebrafish-specific (TGA(G/C)nnnTC) and mammalian (TGA(G/C)nnnGC) consensus sequences were identified, as previously described in (Suzuki *et al.*, 2005) and performed in (Timme-Laragy, et al., 2012). The Nrf2-Maf complex is able to bind to both of these sequences in the zebrafish while maintaining function (Suzuki, et al., 2005). The genomic search was done interrogating sequences identified by UCSC Genome Browser (Zebrafish Sep. 2014 (GRCz10/danRer10) Assembly (http://genome.ucsc.edu/)).

2.11 Statistical Analysis

Statview for Windows (version 5.0.1; SAS Institute, Cary, NC, USA) was used to determine differences among the data. Data were log-normalized and subjected to a two-factor ANOVA for genotype and treatment, or plasmid and treatment. If an ANOVA yielded significance ($p < 0.05$),

Fisher's protected least significant differences test was used as a *post hoc* test. For yolk area measurements, a F-test and T-test were performed in Excel, using a 2-tailed distribution.

3. Results

3.1 The Nrf2a mutant allele encodes a protein deficient in ability to activate transcription via ARE.

To assess the functional consequences of *nrf2a*^{fh318} and *nrf2a*^{fh319} mutations, we measured the ability of these mutants to activate transcription of an antioxidant response element (ARE) reporter gene (luciferase) in comparison to wild-type Nrf2a protein. Both Nrf2a^{fh318} and Nrf2a^{fh319} proteins were expressed strongly in COS-7 cells, as measured by Western blot (Fig. 1A). In the transient transfection assay, wild-type Nrf2a increased luciferase even in the absence of exogenous activator, and there was no additional enhancement in the presence of the Nrf2 activator tBHQ (Fig. 1B). Wild-type Nrf2a activity was repressed by co-transfection of a plasmid expressing zebrafish Keap1a, but only weakly repressed by Keap1b. tBHQ had no effect on the activity of Nrf2a in the presence of Keap1a repression.

In contrast to the wild-type Nrf2a, the transcriptional activity of Nrf2a^{fh318} was greatly diminished, regardless of whether tBHQ was present (Fig. 1B). A small amount of residual activity was evident, and this was eliminated by co-transfection of Keap1a but only slightly affected by Keap1b. The Nrf2a^{fh319} protein retained nearly full transactivation activity that was slightly enhanced by tBHQ (Fig. 1B). Therefore, the Nrf2a^{fh319} mutant zebrafish line was not used in subsequent experiments. Together, these results suggest that the Nrf2a^{fh318} allele encodes a Nrf2a protein that is greatly diminished in activity but retains some residual activity, at least *in vitro*.

3.2 Nrf2a mutants are more sensitive to PCB126 teratogenesis than wildtype eleutheroembryos.

Pericardial edema and craniofacial malformations are some of the best characterized deformities associated with PCB126 and DLC embryotoxicity in fish embryos. To determine whether *nrf2a*$^{fh318/fh318}$ mutants were more or less sensitive than wild type embryos to PCB126 embryotoxicity, we exposed embryos to 2 nM or 5 nM PCB126 for 1 h from 25-26 hpf, and measured malformations at 4 dpf and 5 dpf (Fig 2 and 3, respectively). Pericardial edema and jaw deformities were more severe in *nrf2a*$^{fh318/fh318}$ eleutheroembryos than in wildtype controls when assessed at 4 dpf (Fig 2). At 5 nM PCB126, these deformities are present in only a subset of exposed embryos, and wildtype eleutheroembryos did not have a statistically significant

increase in pericardial edema area at 4 dpf, whereas the mutants exposed to 5 nM PCB126 had nearly twice the pericardial area of controls (Fig. 2D). The mean jaw deformity score was a more sensitive measure of embryotoxicity, with a significant increase in the deformity score at 2 nM in the mutants. A significant increase in jaw deformities was observed in both genotypes at 5 nM (Fig. 2E). At both exposure concentrations, the jaw deformities in the mutants were more severe and more frequent than those in the wildtype eleutheroembryos. However, at 5 dpf, both the *nrf2a* mutant and wildtype eleutheroembryos demonstrated similar pericardial and jaw deformity severity (Fig. 3C, Fig. 3D).

We identified two notable developmental differences between the *nrf2a*$^{fh318/fh318}$ and wildtype controls. First, ventral-dorsal distance, which was used to estimate yolk usage, was significantly lower in *nrf2a*$^{fh318/fh318}$ versus wildtype fish (Figs. 2A, 2B). While the ventral-dorsal distance increased in a PCB dose-dependent manner in both genotypes, reflecting poor yolk sac absorption, it was surprising that the *nrf2a* mutant DMSO control eleutheroembryos had, on average, a significantly shorter dorsal-ventral distance than age-matched wildtype fish, by approximately 8% at 4 dpf (Fig. 2B) At 5 dpf, ventral-dorsal distance between *nrf2a* mutants and wildtype eleutheroembryos remained significantly different (Fig. 3A). To determine if the shorter dorsal-ventral measurements in the mutant fish was due to *nrf2a*$^{fh318/fh318}$ fish laying smaller eggs, we measured the diameter of the yolk in fertilized embryos (3 hpf) from Nrf2a homozygous wildtype or *nrf2a*$^{fh318/fh318}$ adults. Surprisingly, mutants had, on average, larger yolk sac areas than the wildtype embryos ($p < 0.0001$; Fig. 4).

The second notable developmental difference was with respect to the timing of swim bladder inflation. In the mutant fish, only 20% of the DMSO controls had inflated swim bladders at the 4-dpf timepoint, compared to 90% of the wildtype DMSO controls. Treatment with PCB126 effectively prevented swim bladder inflation in a dose-dependent manner among wildtype fish at 4 dpf (25% of embryos treated with 2 nM, and 0% treated with 5 nM; Fig 2C and as previously reported (Jonsson, et al., 2012)). This is in contrast to the *nrf2a* mutant embryos, where none of the PCB-treated embryos had successfully inflated swim bladders at 4 dpf (Fig. 2C). However, interpretation of these data was confounded by a 24-h delay in swim bladder inflation among the *nrf2a*$^{fh318/fh318}$ eleutheroembryos controls. When assessed at 5 dpf, there were no differences in swim bladder inflation between the control wildtype or mutant *nrf2a* genotypes (Fig. 3B). At 5 dpf, 80% of DMSO controls had inflated swim bladders, while only 40% of embryos treated with 2 nM and 0-10% of embryos treated with 5 nM had successfully inflated swim bladders (Fig. 3B).

3.3 Regulation of Ahr pathway gene expression by Nrf2a

To confirm that the embryos had been effectively dosed with PCB126, we measured induction of *cyp1a*, a primary biomarker of ligand activation of the Ahr. There was no significant difference in Cyp1a enzyme activity (*in vivo* EROD activity, data not shown), and no difference in *cyp1a* gene expression between genotypes in the DMSO control (Fig. 5A). There was a significant dose-dependent increase in gene expression of *cyp1a* in response to 2 and 5 nM PCB126 in both genotypes, but the *nrf2a* mutants had nearly double the induction of *cyp1a* compared to wildtype fish.

To determine whether the enhanced *cyp1a* induction by PCB126 was due to differential expression of *ahr* genes, we measured expression of *ahr2* (the ortholog that has been demonstrated to regulate co-planar PCB and TCDD embryotoxicity). Expression of *ahr2* was not significantly different between the two genotypes at 4 dpf. The expression of *ahr2* was induced by PCB126 exposure in a dose-dependent manner and to a similar extent in both mutant and wildtype embryos (Fig. 5B).

Because there have been some reports that *cyp1a* induction can be regulated by the other *ahr* genes, *ahr1a* and *ahr1b,* we also measured expression of these genes. Expression of *ahr1a* was similar in control embryos of the two genotypes, but the magnitude of induction following PCB126 treatment differed between genotypes. *ahr1a* was only inducible in the *nrf2a* wildtype fish (2.6 and 4.3 fold for the 2 nM and 5 nM exposures respectively, Fig. 5C); expression of this gene did not change with PCB126 treatment in the *nrf2a*$^{fh318/fh318}$ eleutheroembryos at 4 dpf. Similarly, expression of *ahr1b* was slightly induced by PCB126 in wild type embryos (2-fold with 5 nM) but was not induced in the *nrf2a* mutants (Fig 5D). Interestingly, the *nrf2a* mutants had significantly lower basal expression (70-75% lower) of *ahr1b* compared to the wildtype fish at this stage.

Basal expression of the two Ahr repressor genes, *ahrra* and *ahrrb,* both tended to be lower in the *nrf2a* mutants, but this was not statistically significant. Both of these genes demonstrated dose-dependent increases in expression in both genotypes with 2 nM and 5 nM PCB126 treatments, but the induction level was greater in the *nrf2a* wildtype fish (Figs. 5E, 5F). Wildtype zebrafish showed a 21.5- and 34.6- fold increase in expression of *ahrra* at the 2 nM and 5 nM PCB126 treatments respectively, compared to 14.5- and 27.5-fold increases in the mutant fish (Fig. 5E). Inducible expression of *ahrrb* was not as high as *ahrra*; wildtype expression increased

10.4 and 23.9-fold in the wildtypes, and 3.2- and 6.8-fold in the mutants, approximately 10-fold lower than *ahrra* expression at these doses of PCB126 (Fig. 5F).

3.4 Regulation of Nrf-family and Keap genes by Nrf2a

The influence of nrf2a function on the expression of other nrf genes was investigated. There were no statistically significant differences in the basal expression of either *nrf1a* or *nrf1b* between the wildtype and *nrf2a* mutant eleutheroembryos (Figs. 6A, 6B). Both genes were upregulated with PCB126 exposure in the wildtype fish only. Expression of *nrf1a* was 2-fold greater in the eleutheroembryos exposed to PCB126 treatment (Fig. 6A). Expression of *nrf1b* was 4-fold higher in the 2 nM PCB126 exposure group, but not significantly different from controls at the 5 nM concentration (Fig. 6B), suggesting an inverted-U-shaped curve. We found no difference in basal expression of *nrf3* between the wildtype and *nrf2a* mutant eleutheroembryos, but there was a significant 2-fold induction of *nrf3* with PCB126 only in the wildtype embryos (Fig. 6D).

To ensure that transcription of *nrf2a* was indeed comparable between the wildtype and mutants, we also measured gene expression of *nrf2a.* There was no significant difference in basal expression between the genotypes, but there was a difference in inducibility by PCB126 (Fig. 6C). The expression of *nrf2a* was significantly up-regulated in response to PCB126 in both genotypes, but this up-regulation was greater in the wildtype eleutheroembryos (1.7-fold). While *nrf2a* expression in the mutant embryos was increased by PCB126 exposure, this increase did not exceed the basal levels in the wildtype eleutheroembryos (Fig. 6C).

Expression of both *keap1a* and *keap1b* genes, the cytosolic repressors of Nrf2a, tended to be lower in the *nrf2a* mutant eleutheroembryos, but this was not statistically significant (Figs. 6E, 6F). Both were inducible by PCB126 in the wildtype but not *nrf2a* mutant eleutheroembryos. Expression of *keap1a* and *keap1b* increased 2- fold in the wildtype embryos at the 2 nM treatment but only 1.5- fold in the 5 nM treatment.

We measured expression of *nrf2b,* a repressive paralog of *nrf2a,* and found a dose-dependent increase only in the mutant embryos exposed to PCB126 (5.2-fold and 6.8-fold at the 2 nM and 5 nM exposures respectively; Fig. 7A). We then measured expression of *hmox1* and *tp53*, two genes negatively regulated by Nrf2b (Timme-Laragy, et al., 2012). Expression of *hmox1* increased 3-fold only in the *nrf2a* wildtype embryos at 2 nM PCB126, but not at 5 nM (Fig. 7B). Expression of *tp53* did not change significantly with PCB126 exposure in either genotype, although there was a significant difference in the expression levels between the two genotypes

with the 5 nM treatment (1.5-fold increase in wildtype and 0.7-fold decrease in Nrf2a mutants; Fig. 7C).

3.5 Measures of oxidative stress responsive genes in PCB126 embryotoxicity

To determine whether a transcriptional response to PCB126-induced oxidative stress was evident in this study, we measured three well-established genes characteristic of an oxidative stress response: *heat shock protein 70 (hsp70), glutathione-s-transferase pi 1 (gstp1)* and *glutamate-cysteine ligase catalytic subunit (gclc).* If PCB126 were causing oxidative stress, it would be expected that these genes would be upregulated in the wildtype embryos exposed to PCB126; however, in these exposures, there was no change in expression of these genes with PCB126 exposure and no difference between the two genotypes (Supplemental Fig. 2).

3.6 Gene targets co-regulated by Ahr and Nrf2

Induction of the genes *gsta1* and *nqo1* can be regulated by both AHR and NRF2 after treatment with TCDD in mice (Yeager, et al., 2009). Interestingly, *nrf2a* mutant eleutheroembryos had higher basal expression of both of these genes, 4-5- fold more *gsta1* and 2-fold higher expression of *nqo1* than the wildtype embryos at the DMSO, 2 nM and 5 nM PCB 126 treatment; however, there was no significant response to PCB126 (Fig. 8).

3.7 Putative AREs can be found across Ahr and Nrf2 target promoters

To determine the potential for Nrf2 to have a direct effect on the abundance and function of the genes, a bioinformatic search for putative mammalian (M) or zebrafish-specific (Z) AREs was performed on all candidate genes. Mammalian and/or zebrafish-specific putative AREs were found in each gene (Table 1). Several genes had AREs within 1000 bp upstream or 100 bp downstream of the transcription start site, often deemed key regulatory zones. These genes include *ahr1b, ahr2, ahrra, ahrrb, cyp1a, gstp1, hmox1, hsp70, keap1a,* and *nrf1b*. A subset of these genes have AREs within 100 bp of the beginning of Exon 1, including *hsp70*, *nrf1b*, *gstp1*, *ahrra*, and *ahr2*.

4. Discussion

NRF2 and AHR have been shown to positively regulate the expression of one another in mammals (Ma, et al., 2004; Miao, et al., 2005; Shin *et al.*, 2007). Nrf2 in both fish and mammals can also regulate its own expression (Kwak *et al.*, 2002; Timme-Laragy, et al., 2012; Williams *et al.*, 2013). In this study, we examined PCB126 embryotoxicity and gene expression during the sensitive period of embryonic development, with a focus on these two important pathways, Ahr and Nrf2. We have also further characterized the *nrf2a* ^{fh318} recessive loss-of-

function mutant fish with respect to some subtle developmental effects and differences in basal gene expression. While these zebrafish mutants have been previously characterized (Mukaigasa, et al., 2012), and demonstrated to be similar to the NRF2 null mouse in some respects (Mukaigasa, et al., 2012), our luciferase data from over-expressed Nrf2a^{fh318} mutant protein suggests that there may be some slight DNA binding activity, at least *in vitro.* Our assessment of the Nrf2a^{319} mutant protein indicated that it maintained effective interactions with the ARE, consistent with earlier results (Mukaigasa, et al., 2012).

Mammalian models lacking NRF2 and zebrafish with either mutated or knocked-down Nrf2a have demonstrated an increased sensitivity to toxicants including TCDD (Lu, et al., 2011), PAHs (Timme-Laragy *et al.*, 2009), and pro-oxidants (Mukaigasa, et al., 2012; Suzuki, et al., 2005; Timme-Laragy, et al., 2012). In the present study, we used relatively low concentrations of PCB126 that were not expected to cause severe and pervasive deformities. Yet, *nrf2a* $^{fh318/fh318}$ fish were found to be more sensitive to PCB126 embryotoxicity, as measured by pericardial edema area and craniofacial malformations; a surprising result was the transient nature of this effect. We show here that at 4 dpf the *nrf2a* mutant embryos have more severe morphological effects of PCB126 exposure (Fig. 2), but by 5 dpf, these effects have largely equalized between the genotypes (Fig. 3).

This study identified subtle developmental differences between the wildtype and *nrf2a* $^{fh318/fh318}$ embryos and eleutheroembryos. There was a one day delay in swim bladder inflation, which is one of the hallmarks of embryotoxicity caused by exposure to PCB126 and other dioxin-like-compounds (DLCs), and a shortened dorsal-ventral measure, reflecting a slightly smaller yolk sac (Figs. 2-4). Since the mutant embryos start out with larger yolks (at 3 hpf) than wildtype embryos, we suggest that this smaller yolk may be due to an increased rate of yolk utilization by the *nrf2a* $^{fh318/fh318}$ embryos, and are conducting a follow-up study to better understand this. While previous studies have demonstrated that NRF2 is not essential for normal development and reproduction in both zebrafish and mice (Chan *et al.*, 1996; Itoh, et al., 1997; Mukaigasa, et al., 2012) some subtle effects in NRF2 mutant mice have been identified. NRF2 -\- mice have defects in liver growth and size (Beyer, et al., 2008), reduced bile duct microbranching (Skoko, et al., 2014), reduced retinal vasculature density (Wei, et al., 2013), and in some genetic backgrounds, a congenital defect resulting in an intrahepatic shunt (Skoko, et al., 2014).

We identified putative AREs throughout the promoter regions of genes involved in the Ahr, Nrf2, and general stress responses (Table 1). Several Ahr targets and pathway genes have putative

AREs in their promoters within 1000 bp upstream or 100 bp downstream of the beginning of Exon 1. These genes include *ahr1b, ahr2, ahrra, ahrrb,* and *cyp1a*. Because of the close proximity of these loci to the TATAA box, it is highly possible that Nrf2 binding in these regions may in some way affect transcriptional activation. Deletion of this region of the *gstp1* gene in zebrafish has been demonstrated to completely eliminate induction by Nrf2a (Suzuki, et al., 2005). Though indirect crosstalk between the Ahr and Nrf2 signaling pathways is likely, it is also possible that Nrf2 may directly activate these genes. However, these are putative AREs and thus confirmation of Nrf2 transcription factor binding and activation of these targets would be required in order to determine whether Nrf2 does activate or repress transcription of these genes. Several other groups have performed ChIP-seq in various tissues and cell lines in order to discern whether basal and/or induced NRF2 has any novel targets in various tissues (Campbell *et al.*, 2013; Chorley *et al.*, 2012; Malhotra, et al., 2010). Though these studies confirmed NRF2 binding to a similar core of genes associated with the antioxidant response, such as those included in glutathione synthesis and phase II metabolism, these studies also identified novel targets for each cell line or tissue.

We identified significant changes in gene expression during development among the *ahr* target genes that were altered in the absence of a fully-functional Nrf2a, with respect to both basal and PCB126-inducible expression (summarized in Table 2). For example, *nrf2a* mutants had nearly double the induction of *cyp1a* compared to wildtype fish in response to PCB126 (Fig.5A). As Ahr activation is directly related to the severity of deformities after exposure to DLCs, this finding concurs with the enhanced severity of deformities observed in these mutants at the 4 dpf timepoint (Fig. 2). However, there are conflicting findings in the literature with regards to the role of Nrf2 in expression of *cyp1a.* In some studies of adult NRF2 knockout mice treated with TCDD, expression of *Cyp1a1* was lower than in wildtype livers (Anwar-Mohamed, et al., 2011), as was expression of *Ahr, Cyp1a1*, and *Cyp1b1* in mouse embryo fibroblasts derived from NRF2 knockout mice (Shin, et al., 2007). Still others found no change in the basal or inducible expression of *Cyp1a1* or *Cyp1a2* in livers of adult NRF2 knockout mice (Aleksunes and Klaassen, 2012; Noda *et al.*, 2003; Yeager, et al., 2009). There may be several reasons for this discrepancy in results pertaining to the basal and inducible expression of *cyp1a* in our study and in the literature overall. There may be differences related to developmental events or the inclusion of whole embryo gene expression compared to isolated adult liver tissues measured in other studies. There may also be differences related to the dose and the inducer used.

The greater induction in *cyp1a* expression in Nrf2a mutants in our study may also be due to concurrent changes in expression of the aryl hydrocarbon receptor repressor (*ahrr*) genes. It is conceivable that the diminished induction in expression of the *ahrr* genes could result in diminished repression of Ahr2 transcriptional activity and subsequently contribute to the enhanced expression of *cyp1a* in the mutants. The molecular mechanism by which Nrf2a affects expression of *ahrra* and *ahrrb* is also unknown and requires further investigation. However, both *ahrr* genes contain putative AREs in their promoters (7 in *ahrra,* and 6 in *ahrrb;* Table 1). For both *ahrra* and *ahrrb*, there is an ARE proximal to the transcription start site, suggesting that they may be directly induced by Nrf2 activation. Increasing PCB concentrations increased *ahrra* and *ahrrb* expression in *nrf2a* mutants, albeit to a significantly lesser degree for *ahrrb (*Fig. 5). To our knowledge, the function of AHRR has not yet been examined in NRF2 knockout mice.

The induction of *cyp1a* in zebrafish is largely regulated by Ahr2, although some studies suggest that Ahr1a, which is not capable of binding to TCDD (Karchner, et al., 2005), may have some role in the endogenous regulation of *cyp1a* (Garner, et al., 2013; Goodale, et al., 2012; Incardona *et al.*, 2006). It has been shown that a knockdown of Ahr1a via morpholino exacerbated cardiac toxicity of PCB126 and increased Cyp1a activity (EROD activity) in exposed embryos (Garner, et al., 2013). A knockdown of Ahr1b showed no such visible or quantitative effect on PCB126 toxicity (Garner, et al., 2013). In another study, TCDD was unable to induce *ahr1a* expression in zebrafish larvae at 48 or 72 hpf (Karchner, et al., 2005). In the present study at 4 dpf, *ahr1a* and *ahr1b* were expressed more highly in wild-type embryos than mutants and there was a dose-dependent increase in expression with increasing concentration of PCBs in wild-type embryos (Fig. 5). Interestingly, there was no induction in the mutant embryos. This would suggest that Nrf2 activation may be necessary for upregulation of *ahr1a* and *ahr1b;* the presence of putative AREs in their promoters provides additional support for this mechanism.

It is important to note here that not all Ahr target genes responded in a similar manner in this study (Table 2). For example, there are conflicting patterns with *cyp1a* being more inducible in the *nrf2a* mutants, while the *ahrr* genes were less inducible. This has also been reported by others (Yeager, et al., 2009) (Nukaya *et al.*, 2010), and reflects the complex nature of gene network interactions that will require further study to dissect the contribution of Nrf2.

Nqo1 has been categorized as part of the mammalian "AhR battery of genes." However, Ahr crosstalk with Nrf2 may be necessary for proper induction of Nqo1 (Yeager et al, 2009, Wang et al, 2013). NRF2-null mice have shown a decrease in NQO1 protein when exposed to 3-MC, an inducer of Phase 1 genes, and BHA, an inducer of phase 2 genes (Jin *et al.*, 2014). Likewise, *Gstp*, a gene typically associated with the "Nrf2 battery of genes", experienced a decrease in protein expression when treated with BHA in AHR-null mutant mice, thus suggesting a relationship between Nrf2 and Ahr in the regulation of these genes (Noda, et al., 2003). Our results show an unexpected increase in basal expression and induction of *nqo1*, and a lack of induction of *gstp1* when treated with low concentrations of the Ahr agonist, PCB126, in the *nrf2a* mutants (Fig 8). Though our *nqo1* expression pattern is different from mammalian studies, it is consistent with what has been found in the zebrafish model using the Nrf2 activator tBHQ, the Ahr activator BaP, or water soluble oil fractions (Corrales *et al.*, 2014; dos Anjos *et al.*, 2011; Hahn, et al., 2014).

In the current study, we found that some Phase II genes we measured (*nqo1, gsta1*) were expressed at higher levels in the *nrf2a* mutant fish compared to wildtype controls, with no significant change in expression associated with PCB126 exposure in either genotype (Fig. 8). This is contrary to what has been found for most other Phase II genes, whose expression in adult mice has been shown to increase with NRF2 activation, and decrease in the NRF2 null mouse model, the exception being *Sult1a1*, which decreased with Nrf2 activation (Wu *et al.*, 2012). Although both NQO1 and GSTa1 are NRF2 targets in mammalian systems, there are contradictory data concerning whether this is true in zebrafish (Hahn, et al., 2014; Kobayashi, et al., 2002; Nakajima *et al.*, 2011). Other genes have been found to be over-expressed in Nrf2a$^{fh318/fh318}$ larvae, including *gpx1b* (Mukaigasa, et al., 2012). This upregulation may be compensatory to counteract the reduced antioxidant response capacity in the mutant embryos. It is important in interpreting our results to keep in mind the nature of this Nrf2a mutation; all other functional elements of the Nrf2a protein remain intact, enabling full interactions with Keap1 and other proteins. This is inherently different from the NRF2 null mouse, in which the much of the gene was removed and no functional NRF2 protein synthesized (Chan, et al., 1996).

Other members of the *nrf* gene family are capable of binding to AREs and regulating gene expression, and mammalian NRF1 and NRF2 have been shown to have some overlap in the sets of genes that they regulate (Ohtsuji, et al., 2008). We therefore considered the possibility that in the *nrf2a* mutant embryos, other *nrf* family members may be compensating for the deficient transcriptional activity of Nrf2a. Previous research demonstrated that the inducible, but

not basal, expression of *nrf1a* and *nrf1b* following exposure to *tert* butylhydroperoxide was dependent on the presence of Nrf2a (Williams, et al., 2013). However, we found no differences in the basal expression of these genes, although there was a trend towards a reduced basal expression in *nrf1a,* and *nrf1b* (Fig. 6). Williams et al. identified ARE and XREs in the promoters of the Nrf family members (*nrf1a, nrf1b, nrf2b, nrf3, nfe2*), and with the exception of *nrf3,* expression each of these can be upregulated by tert butylhydroperoxide (Williams, et al., 2013). In Nrf2a-morpholino embryos, the upregulation of *nfe2, nrf1a,* and *nrf1b* was either lost or greatly diminished, but the upregulation of *nrf3* was enhanced by Nrf2a knockdown. Here we found that these *nrf* family genes, as well as the cytosolic repressor proteins *keap1a* and *keap1b* were inducible by PCB126, but only in the wildtype eleutheroembryos (Fig. 6), indicating that Nrf2a is an important contributor to this response.

Our previous studies of the novel *nrf2a* gene paralog, *nrf2b,* identified a role for this gene in the negative transcriptional regulation of *tp53* and *hmox1,* and also showed that inducible expression of both *nrf2a* and *nrf2b* was dependent on Ahr2 (Timme-Laragy, et al., 2012). We expand upon that finding here, and have shown that inducible expression of *nrf2b* with PCB126 is also dependent on Nrf2a (Fig. 7). Our data also provides support for the previously identified negative transcriptional regulation of *hmox1* by Nrf2b: the induction of *hmox1* by PCB126 in the wildtype embryos was not observed in the *nrf2a* mutant embryos, and this was correlated with the increased expression of *nrf2b.*

It is well-established that PCB126 is capable of causing oxidative stress in mammals, cell culture, and fish models (Arzuaga *et al.*, 2006; Chen, 2010; Hassoun and Periandri-Steinberg, 2010; Park *et al.*, 2010). For example, Schlezinger et al. demonstrated that ROS can be generated from PCB126 exposure via the uncoupling of the catalytic cycle of Cyp1a (Schlezinger, et al., 2006). Other groups have demonstrated oxidative stress resulting from PCB126 exposure in zebrafish embryos, including a transcriptional oxidative stress response; however, the concentrations used in those studies were 100 nM (Na *et al.*, 2009) and 64 and 128 µg/L (Liu *et al.*, 2014) which are drastically greater than the highest dose used in this study (5 nM or 7 µg/L). ROS generated at low PCB126 concentrations may be difficult to detect, and may not have been captured in our experimental design. Or perhaps oxidative stress may not be a primary factor contributing to the deformities caused by low concentrations of PCB126. Another point of consideration is that *nrf2a* $^{fh318/fh318}$ fish have been shown to be more sensitive to some, but not all, sources of ROS and electrophiles. For example, while *nrf2a* mutants were more sensitive to peroxides and acetaminophen, they were only moderately more sensitive to

paraquat, and not more sensitive to menadione (Mukaigasa, et al., 2012). The only indication of an oxidative stress response in our data was the upregulation of *hmox1* by PCB126; otherwise we did not identify changes in gene expression that would be typical of an oxidative stress response (Hahn, et al., 2014). This study used low concentrations of PCB126, yet still demonstrated an important role for Nrf2a in the transcriptional response and embryotoxicity. The mechanistic function of Nrf2a in these processes is not entirely clear, but these studies suggest a noncanonical role of Nrf2a, or that interaction with the Ahr itself may be important. Wang et al. provided evidence suggesting that AHR upregulated the transcription of *Nrf2* and formed protein complexes with both NRF2 and KEAP1 that contributed to the stability of NRF2 and subsequent ARE-activation (Wang, et al., 2013). Thus, regulation of Nrf2 by Ahr could occur via transcriptional regulation as well as direct protein-protein interactions.

In the age of transcriptomics, it is becoming increasingly important to understand the role of crosstalk between transcriptional pathways. It is no longer effective to think of pathways as simply linear models; rather, they need to be examined as networks that interact with each other. Studying the transcriptional regulators of such gene networks, and their interactions, will be important to the field of toxicology in understanding toxicant responses and predicting toxicity.

5. Conclusions

Here we have taken a targeted candidate gene approach to focus on important genes in the Nrf2a and Ahr2 pathways. We have shown complex interactions between these regulatory pathways, and resulting consequences for PCB126 embryotoxicity. We have suggested that the Nrf2a fh318 mutant allelic variant may be slightly functional at the transcriptional level, at least *in vitro*. We identified some important developmental differences between the mutants and the wildtype embryos, and a transient increase in sensitivity to PCB126 embryotoxicity in the *nrf2a* mutants. This is correlated with a higher induction of *cyp1a* in these mutants. Finally, we demonstrated that expression of members of the *ahr* and *nrf2* gene families are affected by Nrf2a. These findings will have important consequences for the use of these mutant fish by others, and also contribute to our understanding of crosstalk between two pathways that are important to the study of toxicology.

Supplemental Data

Supplemental Table 1. List of qPCR primers, melting temperature, and sources.

Supplemental Figure 1. Protein alignment of the translated *nrf2a* ^{fh318} allele with other Nrf2a protein sequences.

Supplemental Fig.2. . Quantitative real-time PCR measures for oxidative stress response genes in *nrf2a* wildtype and fh318 mutant eleutheroembryos at 4 dpf.

[These figure legends are shown at the end of the paper
]

Funding

University of Massachusetts Amherst Commonwealth Honors College Research grant (to M.R.), National Institutes of Health grants R01ES016366 (MEH), R01ES006272 (MEH), and F32ES017585 (ART-L).

Acknowledgements

We would like to acknowledge the excellent fish care provided by Brandy Joyce and Gale Clark at WHOI, and by Karen Melendez, Derek Luthi, Sonia Filipczak, Marjorie Marin, Jiali Xu, Christopher Sparages, Shana Fleishman, Kaylee-Anna Williams, Katrina Borofski, and Gabriella McClellen at UMASS.

References

Aleksunes, L. M., and Klaassen, C. D. (2012). Coordinated regulation of hepatic phase I and II drug-metabolizing genes and transporters using AhR-, CAR-, PXR-, PPARalpha-, and Nrf2-null mice. *Drug metabolism and disposition: the biological fate of chemicals* **40**(7), 1366-79, 10.1124/dmd.112.045112.

Alexeyenko, A., Wassenberg, D. M., Lobenhofer, E. K., Yen, J., Linney, E., Sonnhammer, E. L., and Meyer, J. N. (2010). Dynamic zebrafish interactome reveals transcriptional mechanisms of dioxin toxicity. *PloS one* **5**(5), e10465, 10.1371/journal.pone.0010465.

Andreasen, E. A., Spitsbergen, J. M., Tanguay, R. L., Stegeman, J. J., Heideman, W., and Peterson, R. E. (2002). Tissue-specific expression of AHR2, ARNT2, and CYP1A in zebrafish embryos and larvae: effects of developmental stage and 2,3,7,8-tetrachlorodibenzo-p-dioxin exposure. *Toxicological sciences : an official journal of the Society of Toxicology* **68**(2), 403-19.

Anwar-Mohamed, A., Degenhardt, O. S., El Gendy, M. A., Seubert, J. M., Kleeberger, S. R., and El-Kadi, A. O. (2011). The effect of Nrf2 knockout on the constitutive expression of drug

metabolizing enzymes and transporters in C57Bl/6 mice livers. *Toxicology in vitro : an international journal published in association with BIBRA* **25**(4), 785-95, 10.1016/j.tiv.2011.01.014.

Arzuaga, X., Wassenberg, D., Di Giulio, R., and Elskus, A. (2006). The chlorinated AHR ligand 3,3',4,4',5-pentachlorobiphenyl (PCB126) promotes reactive oxygen species (ROS) production during embryonic development in the killifish (Fundulus heteroclitus). *Aquatic toxicology (Amsterdam, Netherlands)* **76**(1), 13-23, 10.1016/j.aquatox.2005.07.013.

Beyer, T. A., Xu, W., Teupser, D., auf dem Keller, U., Bugnon, P., Hildt, E., Thiery, J., Kan, Y. W., and Werner, S. (2008). Impaired liver regeneration in Nrf2 knockout mice: role of ROS-mediated insulin/IGF-1 resistance. *The EMBO journal* **27**(1), 212-23, 10.1038/sj.emboj.7601950.

Billiard, S. M., Timme-Laragy, A. R., Wassenberg, D. M., Cockman, C., and Di Giulio, R. T. (2006). The role of the aryl hydrocarbon receptor pathway in mediating synergistic developmental toxicity of polycyclic aromatic hydrocarbons to zebrafish. *Toxicological sciences : an official journal of the Society of Toxicology* **92**(2), 526-36, 10.1093/toxsci/kfl011.

Bock, K. W. (2013). The human Ah receptor: hints from dioxin toxicities to deregulated target genes and physiological functions. *Biological chemistry* **394**(6), 729-39, 10.1515/hsz-2012-0340.

Bryan, H. K., Olayanju, A., Goldring, C. E., and Park, B. K. (2013). The Nrf2 cell defence pathway: Keap1-dependent and -independent mechanisms of regulation. *Biochemical pharmacology* **85**(6), 705-17, 10.1016/j.bcp.2012.11.016.

Campbell, M. R., Karaca, M., Adamski, K. N., Chorley, B. N., Wang, X., and Bell, D. A. (2013). Novel hematopoietic target genes in the NRF2-mediated transcriptional pathway. *Oxidative medicine and cellular longevity* **2013**, 120305, 10.1155/2013/120305.

Chan, K., Lu, R., Chang, J. C., and Kan, Y. W. (1996). NRF2, a member of the NFE2 family of transcription factors, is not essential for murine erythropoiesis, growth, and development. *Proceedings of the National Academy of Sciences of the United States of America* **93**(24), 13943-8.

Chen, F. (2010). Induction of oxidative stress and cytotoxicity by PCB126 in JEG-3 human choriocarcinoma cells. *Journal of environmental science and health. Part A, Toxic/hazardous substances & environmental engineering* **45**(8), 932-7, 10.1080/10934521003772311.

Chorley, B. N., Campbell, M. R., Wang, X., Karaca, M., Sambandan, D., Bangura, F., Xue, P., Pi, J., Kleeberger, S. R., and Bell, D. A. (2012). Identification of novel NRF2-regulated genes by ChIP-Seq: influence on retinoid X receptor alpha. *Nucleic acids research* **40**(15), 7416-7429, 10.1093/nar/gks409.

Corrales, J., Fang, X., Thornton, C., Mei, W., Barbazuk, W. B., Duke, M., Scheffler, B. E., and Willett, K. L. (2014). Effects on specific promoter DNA methylation in zebrafish embryos and larvae following benzo[a]pyrene exposure. *Comparative biochemistry and physiology. Toxicology & pharmacology : CBP* **163**, 37-46, 10.1016/j.cbpc.2014.02.005.

Cullinan, S. B., Gordan, J. D., Jin, J., Harper, J. W., and Diehl, J. A. (2004). The Keap1-BTB protein is an adaptor that bridges Nrf2 to a Cul3-based E3 ligase: oxidative stress sensing by a Cul3-Keap1 ligase. *Molecular and cellular biology* **24**(19), 8477-86, 10.1128/mcb.24.19.8477-8486.2004.

Dalton, T. P., Puga, A., and Shertzer, H. G. (2002). Induction of cellular oxidative stress by aryl hydrocarbon receptor activation. *Chemico-biological interactions* **141**(1-2), 77-95.

Denison, M. S., Soshilov, A. A., He, G., DeGroot, D. E., and Zhao, B. (2011). Exactly the same but different: promiscuity and diversity in the molecular mechanisms of action of the aryl hydrocarbon (dioxin) receptor. *Toxicological sciences : an official journal of the Society of Toxicology* **124**(1), 1-22, 10.1093/toxsci/kfr218.

dos Anjos, N. A., Schulze, T., Brack, W., Val, A. L., Schirmer, K., and Scholz, S. (2011). Identification and evaluation of cyp1a transcript expression in fish as molecular biomarker for petroleum contamination in tropical fresh water ecosystems. *Aquatic toxicology (Amsterdam, Netherlands)* **103**(1-2), 46-52, 10.1016/j.aquatox.2011.02.004.

Garner, L. V., Brown, D. R., and Di Giulio, R. T. (2013). Knockdown of AHR1A but not AHR1B exacerbates PAH and PCB-126 toxicity in zebrafish (Danio rerio) embryos. *Aquatic toxicology (Amsterdam, Netherlands)* **142-143**, 336-46, 10.1016/j.aquatox.2013.09.007.

Gillardin, V., Silvestre, F., Dieu, M., Delaive, E., Raes, M., Thome, J. P., and Kestemont, P. (2009). Protein expression profiling in the African clawed frog Xenopus laevis tadpoles exposed to the polychlorinated biphenyl mixture aroclor 1254. *Molecular & cellular proteomics : MCP* **8**(4), 596-611, 10.1074/mcp.M800323-MCP200.

Goodale, B. C., La Du, J. K., Bisson, W. H., Janszen, D. B., Waters, K. M., and Tanguay, R. L. (2012). AHR2 mutant reveals functional diversity of aryl hydrocarbon receptors in zebrafish. *PloS one* **7**(1), e29346, 10.1371/journal.pone.0029346.

Hahn, M. E., Karchner, S. I., Evans, B. R., Franks, D. G., Merson, R. R., and Lapseritis, J. M. (2006). Unexpected diversity of aryl hydrocarbon receptors in non-mammalian vertebrates: insights from comparative genomics. *Journal of experimental zoology. Part A, Comparative experimental biology* **305**(9), 693-706, 10.1002/jez.a.323.

Hahn, M. E., McArthur, A. G., Karchner, S. I., Franks, D. G., Jenny, M. J., Timme-Laragy, A. R., Stegeman, J. J., Woodin, B. R., Cipriano, M. J., and Linney, E. (2014). The transcriptional response to oxidative stress during vertebrate development: effects of tert-butylhydroquinone and 2,3,7,8-tetrachlorodibenzo-p-dioxin. *PloS one* **9**(11), e113158, 10.1371/journal.pone.0113158.

Hahn, M. E., Timme-Laragy, A. R., Karchner, S. I., and Stegeman, J. J. (2015). Nrf2 and Nrf2-related proteins in development and developmental toxicity:Insights from studies in zebrafish (danio rerio). *Free radical biology & medicine* doi: 10.1016/j.freeradbiomed.2015.06.022, 10.1016/j.freeradbiomed.2015.06.022.

Harbeitner, R. C., Hahn, M. E., and Timme-Laragy, A. R. (2013). Differential sensitivity to pro-oxidant exposure in two populations of killifish (Fundulus heteroclitus). *Ecotoxicology* **22**(2), 387-401, 10.1007/s10646-012-1033-x.

Hassoun, E. A., and Periandri-Steinberg, S. (2010). Assessment of the roles of antioxidant enzymes and glutathione in 3,3',4,4',5-Pentachlorobiphenyl (PCB 126)-induced oxidative stress in the brain tissues of rats after subchronic exposure. *Toxicological and environmental chemistry* **92**(2), 301, 10.1080/02772240902846660.

Incardona, J. P., Day, H. L., Collier, T. K., and Scholz, N. L. (2006). Developmental toxicity of 4-ring polycyclic aromatic hydrocarbons in zebrafish is differentially dependent on AH receptor isoforms and hepatic cytochrome P4501A metabolism. *Toxicology and applied pharmacology* **217**(3), 308-21, 10.1016/j.taap.2006.09.018.

Itoh, K., Chiba, T., Takahashi, S., Ishii, T., Igarashi, K., Katoh, Y., Oyake, T., Hayashi, N., Satoh, K., Hatayama, I., Yamamoto, M., and Nabeshima, Y. (1997). An Nrf2/small Maf heterodimer mediates the induction of phase II detoxifying enzyme genes through antioxidant response elements. *Biochemical and biophysical research communications* **236**(2), 313-22.

Jin, Y., Miao, W., Lin, X., Pan, X., Ye, Y., Xu, M., and Fu, Z. (2014). Acute exposure to 3-methylcholanthrene induces hepatic oxidative stress via activation of the Nrf2/ARE signaling pathway in mice. *Environmental toxicology* **29**(12), 1399-408, 10.1002/tox.21870.

Jones, D. P. (2006). Redefining oxidative stress. *Antioxidants & redox signaling* **8**(9-10), 1865-79, 10.1089/ars.2006.8.1865.

Jonsson, M. E., Jenny, M. J., Woodin, B. R., Hahn, M. E., and Stegeman, J. J. (2007). Role of AHR2 in the expression of novel cytochrome P450 1 family genes, cell cycle genes, and

morphological defects in developing zebra fish exposed to 3,3',4,4',5-pentachlorobiphenyl or 2,3,7,8-tetrachlorodibenzo-p-dioxin. *Toxicological sciences : an official journal of the Society of Toxicology* **100**(1), 180-93, 10.1093/toxsci/kfm207.

Jonsson, M. E., Kubota, A., Timme-Laragy, A. R., Woodin, B., and Stegeman, J. J. (2012). Ahr2-dependence of PCB126 effects on the swim bladder in relation to expression of CYP1 and cox-2 genes in developing zebrafish. *Toxicology and applied pharmacology* **265**(2), 166-74, 10.1016/j.taap.2012.09.023.

Karchner, S. I., Franks, D. G., and Hahn, M. E. (2005). AHR1B, a new functional aryl hydrocarbon receptor in zebrafish: tandem arrangement of ahr1b and ahr2 genes. *The Biochemical journal* **392**(Pt 1), 153-61, 10.1042/BJ20050713.

Kensler, T. W., Wakabayashi, N., and Biswal, S. (2007). Cell survival responses to environmental stresses via the Keap1-Nrf2-ARE pathway. *Annual review of pharmacology and toxicology* **47**, 89-116, 10.1146/annurev.pharmtox.46.120604.141046.

Kimmel, C. B., Ballard, W. W., Kimmel, S. R., Ullmann, B., and Schilling, T. F. (1995). Stages of embryonic development of the zebrafish. *Developmental dynamics : an official publication of the American Association of Anatomists* **203**(3), 253-310, 10.1002/aja.1002030302.

King-Heiden, T. C., Mehta, V., Xiong, K. M., Lanham, K. A., Antkiewicz, D. S., Ganser, A., Heideman, W., and Peterson, R. E. (2012). Reproductive and developmental toxicity of dioxin in fish. *Molecular and cellular endocrinology* **354**(1-2), 121-38, 10.1016/j.mce.2011.09.027.

Kobayashi, M., Itoh, K., Suzuki, T., Osanai, H., Nishikawa, K., Katoh, Y., Takagi, Y., and Yamamoto, M. (2002). Identification of the interactive interface and phylogenic conservation of the Nrf2-Keap1 system. *Genes to cells : devoted to molecular & cellular mechanisms* **7**(8), 807-20.

Kwak, M. K., Itoh, K., Yamamoto, M., and Kensler, T. W. (2002). Enhanced expression of the transcription factor Nrf2 by cancer chemopreventive agents: role of antioxidant response element-like sequences in the nrf2 promoter. *Molecular and cellular biology* **22**(9), 2883-92.

Lanham, K. A., Plavicki, J., Peterson, R. E., and Heideman, W. (2014). Cardiac myocyte-specific AHR activation phenocopies TCDD-induced toxicity in zebrafish. *Toxicological sciences : an official journal of the Society of Toxicology* **141**(1), 141-54, 10.1093/toxsci/kfu111.

Li, L., Kobayashi, M., Kaneko, H., Nakajima-Takagi, Y., Nakayama, Y., and Yamamoto, M. (2008). Molecular evolution of Keap1. Two Keap1 molecules with distinctive intervening region structures are conserved among fish. *The Journal of biological chemistry* **283**(6), 3248-55, 10.1074/jbc.M708702200.

Liu, H., Nie, F. H., Lin, H. Y., Ma, Y., Ju, X. H., Chen, J. J., and Gooneratne, R. (2014). Developmental toxicity, oxidative stress, and related gene expression induced by dioxin-like PCB 126 in zebrafish (Danio rerio). *Environmental toxicology* doi: 10.1002/tox.22044, 10.1002/tox.22044.

Lo, R., and Matthews, J. (2013). The aryl hydrocarbon receptor and estrogen receptor alpha differentially modulate nuclear factor erythroid-2-related factor 2 transactivation in MCF-7 breast cancer cells. *Toxicology and applied pharmacology* **270**(2), 139-48, 10.1016/j.taap.2013.03.029.

Lu, H., Cui, W., and Klaassen, C. D. (2011). Nrf2 protects against 2,3,7,8-tetrachlorodibenzo-p-dioxin (TCDD)-induced oxidative injury and steatohepatitis. *Toxicology and applied pharmacology* **256**(2), 122-35, 10.1016/j.taap.2011.07.019.

Ma, Q., Kinneer, K., Bi, Y., Chan, J. Y., and Kan, Y. W. (2004). Induction of murine NAD(P)H:quinone oxidoreductase by 2,3,7,8-tetrachlorodibenzo-p-dioxin requires the

CNC (cap 'n' collar) basic leucine zipper transcription factor Nrf2 (nuclear factor erythroid 2-related factor 2): cross-interaction between AhR (aryl hydrocarbon receptor) and Nrf2 signal transduction. *The Biochemical journal* **377**(Pt 1), 205-13, 10.1042/BJ20031123.

Malhotra, D., Portales-Casamar, E., Singh, A., Srivastava, S., Arenillas, D., Happel, C., Shyr, C., Wakabayashi, N., Kensler, T. W., Wasserman, W. W., and Biswal, S. (2010). Global mapping of binding sites for Nrf2 identifies novel targets in cell survival response through ChIP-Seq profiling and network analysis. *Nucleic acids research* **38**(17), 5718-34, 10.1093/nar/gkq212.

Miao, W., Hu, L., Scrivens, P. J., and Batist, G. (2005). Transcriptional regulation of NF-E2 p45-related factor (NRF2) expression by the aryl hydrocarbon receptor-xenobiotic response element signaling pathway: direct cross-talk between phase I and II drug-metabolizing enzymes. *The Journal of biological chemistry* **280**(21), 20340-8, 10.1074/jbc.M412081200.

Mukaigasa, K., Nguyen, L. T., Li, L., Nakajima, H., Yamamoto, M., and Kobayashi, M. (2012). Genetic evidence of an evolutionarily conserved role for Nrf2 in the protection against oxidative stress. *Molecular and cellular biology* **32**(21), 4455-61, 10.1128/mcb.00481-12.

Na, Y. R., Seok, S. H., Baek, M. W., Lee, H. Y., Kim, D. J., Park, S. H., Lee, H. K., and Park, J. H. (2009). Protective effects of vitamin E against 3,3',4,4',5-pentachlorobiphenyl (PCB126) induced toxicity in zebrafish embryos. *Ecotoxicology and environmental safety* **72**(3), 714-9, 10.1016/j.ecoenv.2008.09.015.

Nakajima, H., Nakajima-Takagi, Y., Tsujita, T., Akiyama, S., Wakasa, T., Mukaigasa, K., Kaneko, H., Tamaru, Y., Yamamoto, M., and Kobayashi, M. (2011). Tissue-restricted expression of Nrf2 and its target genes in zebrafish with gene-specific variations in the induction profiles. *PloS one* **6**(10), e26884, 10.1371/journal.pone.0026884.

Nebert, D. W., Roe, A. L., Dieter, M. Z., Solis, W. A., Yang, Y., and Dalton, T. P. (2000). Role of the aromatic hydrocarbon receptor and [Ah] gene battery in the oxidative stress response, cell cycle control, and apoptosis. *Biochemical pharmacology* **59**(1), 65-85.

Niture, S. K., Khatri, R., and Jaiswal, A. K. (2014). Regulation of Nrf2-an update. *Free radical biology & medicine* **66**, 36-44, 10.1016/j.freeradbiomed.2013.02.008.

Noda, S., Harada, N., Hida, A., Fujii-Kuriyama, Y., Motohashi, H., and Yamamoto, M. (2003). Gene expression of detoxifying enzymes in AhR and Nrf2 compound null mutant mouse. *Biochemical and biophysical research communications* **303**(1), 105-11.

Nukaya, M., Lin, B. C., Glover, E., Moran, S. M., Kennedy, G. D., and Bradfield, C. A. (2010). The aryl hydrocarbon receptor-interacting protein (AIP) is required for dioxin-induced hepatotoxicity but not for the induction of the Cyp1a1 and Cyp1a2 genes. *The Journal of biological chemistry* **285**(46), 35599-605, 10.1074/jbc.M110.132043.

Ohtsuji, M., Katsuoka, F., Kobayashi, A., Aburatani, H., Hayes, J. D., and Yamamoto, M. (2008). Nrf1 and Nrf2 play distinct roles in activation of antioxidant response element-dependent genes. *The Journal of biological chemistry* **283**(48), 33554-62, 10.1074/jbc.M804597200.

Park, S. H., Jang, J. H., Chen, C. Y., Na, H. K., and Surh, Y. J. (2010). A formulated red ginseng extract rescues PC12 cells from PCB-induced oxidative cell death through Nrf2-mediated upregulation of heme oxygenase-1 and glutamate cysteine ligase. *Toxicology* **278**(1), 131-9, 10.1016/j.tox.2010.04.003.

Prasch, A. L., Teraoka, H., Carney, S. A., Dong, W., Hiraga, T., Stegeman, J. J., Heideman, W., and Peterson, R. E. (2003). Aryl hydrocarbon receptor 2 mediates 2,3,7,8-tetrachlorodibenzo-p-dioxin developmental toxicity in zebrafish. *Toxicological sciences : an official journal of the Society of Toxicology* **76**(1), 138-50, 10.1093/toxsci/kfg202.

Schlezinger, J. J., Keller, J., Verbrugge, L. A., and Stegeman, J. J. (2000). 3,3',4,4'-Tetrachlorobiphenyl oxidation in fish, bird and reptile species: relationship to cytochrome

P450 1A inactivation and reactive oxygen production. *Comparative biochemistry and physiology. Toxicology & pharmacology : CBP* **125**(3), 273-86.

Schlezinger, J. J., Struntz, W. D., Goldstone, J. V., and Stegeman, J. J. (2006). Uncoupling of cytochrome P450 1A and stimulation of reactive oxygen species production by co-planar polychlorinated biphenyl congeners. *Aquatic toxicology (Amsterdam, Netherlands)* **77**(4), 422-32, 10.1016/j.aquatox.2006.01.012.

Senft, A. P., Dalton, T. P., Nebert, D. W., Genter, M. B., Puga, A., Hutchinson, R. J., Kerzee, J. K., Uno, S., and Shertzer, H. G. (2002). Mitochondrial reactive oxygen production is dependent on the aromatic hydrocarbon receptor. *Free radical biology & medicine* **33**(9), 1268-78.

Shin, S., Wakabayashi, N., Misra, V., Biswal, S., Lee, G. H., Agoston, E. S., Yamamoto, M., and Kensler, T. W. (2007). NRF2 modulates aryl hydrocarbon receptor signaling: influence on adipogenesis. *Molecular and cellular biology* **27**(20), 7188-97, 10.1128/MCB.00915-07.

Skoko, J. J., Wakabayashi, N., Noda, K., Kimura, S., Tobita, K., Shigemura, N., Tsujita, T., Yamamoto, M., and Kensler, T. W. (2014). Loss of Nrf2 in mice evokes a congenital intrahepatic shunt that alters hepatic oxygen and protein expression gradients and toxicity. *Toxicological sciences : an official journal of the Society of Toxicology* **141**(1), 112-9, 10.1093/toxsci/kfu109.

Suzuki, T., Takagi, Y., Osanai, H., Li, L., Takeuchi, M., Katoh, Y., Kobayashi, M., and Yamamoto, M. (2005). Pi class glutathione S-transferase genes are regulated by Nrf 2 through an evolutionarily conserved regulatory element in zebrafish. *The Biochemical journal* **388**(Pt 1), 65-73, 10.1042/bj20041860.

Tijet, N., Boutros, P. C., Moffat, I. D., Okey, A. B., Tuomisto, J., and Pohjanvirta, R. (2006). Aryl hydrocarbon receptor regulates distinct dioxin-dependent and dioxin-independent gene batteries. *Molecular pharmacology* **69**(1), 140-53, 10.1124/mol.105.018705.

Timme-Laragy, A. R., Karchner, S. I., Franks, D. G., Jenny, M. J., Harbeitner, R. C., Goldstone, J. V., McArthur, A. G., and Hahn, M. E. (2012). Nrf2b, novel zebrafish paralog of oxidant-responsive transcription factor NF-E2-related factor 2 (NRF2). *The Journal of biological chemistry* **287**(7), 4609-27, 10.1074/jbc.M111.260125.

Timme-Laragy, A. R., Van Tiem, L. A., Linney, E. A., and Di Giulio, R. T. (2009). Antioxidant responses and NRF2 in synergistic developmental toxicity of PAHs in zebrafish. *Toxicological sciences : an official journal of the Society of Toxicology* **109**(2), 217-27, 10.1093/toxsci/kfp038.

Wakabayashi, N., Slocum, S. L., Skoko, J. J., Shin, S., and Kensler, T. W. (2010). When NRF2 talks, who's listening? *Antioxidants & redox signaling* **13**(11), 1649-63, 10.1089/ars.2010.3216.

Wang, L., He, X., Szklarz, G. D., Bi, Y., Rojanasakul, Y., and Ma, Q. (2013). The aryl hydrocarbon receptor interacts with nuclear factor erythroid 2-related factor 2 to mediate induction of NAD(P)H:quinoneoxidoreductase 1 by 2,3,7,8-tetrachlorodibenzo-p-dioxin. *Archives of biochemistry and biophysics* **537**(1), 31-8, 10.1016/j.abb.2013.06.001.

Wei, Y., Gong, J., Thimmulappa, R. K., Kosmider, B., Biswal, S., and Duh, E. J. (2013). Nrf2 acts cell-autonomously in endothelium to regulate tip cell formation and vascular branching. *Proceedings of the National Academy of Sciences of the United States of America* **110**(41), E3910-8, 10.1073/pnas.1309276110.

Williams, L. M., Timme-Laragy, A. R., Goldstone, J. V., McArthur, A. G., Stegeman, J. J., Smolowitz, R. M., and Hahn, M. E. (2013). Developmental expression of the Nfe2-related factor (Nrf) transcription factor family in the zebrafish, Danio rerio. *PloS one* **8**(10), e79574, 10.1371/journal.pone.0079574.

Wu, K. C., Cui, J. Y., and Klaassen, C. D. (2012). Effect of graded Nrf2 activation on phase-I and -II drug metabolizing enzymes and transporters in mouse liver. *PloS one* **7**(7), e39006, 10.1371/journal.pone.0039006.
Yeager, R. L., Reisman, S. A., Aleksunes, L. M., and Klaassen, C. D. (2009). Introducing the "TCDD-inducible AhR-Nrf2 gene battery". *Toxicological sciences : an official journal of the Society of Toxicology* **111**(2), 238-46, 10.1093/toxsci/kfp115.
Yoshioka, W., Peterson, R. E., and Tohyama, C. (2011). Molecular targets that link dioxin exposure to toxicity phenotypes. *The Journal of steroid biochemistry and molecular biology* **127**(1-2), 96-101, 10.1016/j.jsbmb.2010.12.005.

Footnotes

Nomenclature: *nrf* is a commonly used notation for NF-E2-related factor genes, which are officially designated as *nfe2l* (NF-E2-like). For example, *nrf2a* is officially designated as *nfe2l2a*. Throughout the paper, we use the more common *nrf* designation. Otherwise, we utilize the approved format for designating genes and proteins (see the ZFIN Zebrafish Nomenclature Web site). Human genes and proteins are designated using all capitals (*NRF2* and NRF2, respectively), rodent genes and proteins as *Nrf2* and NRF2 respectively, whereas zebrafish genes are designated *nrf2* and Nrf2 for genes and proteins, respectively. When not referring to a specific species, we have used the zebrafish notation as a default format.

Figure legends

Fig. 1. Activation of ARE-driven luciferase reporter by Nrf2a mutant alleles *in vitro.* COS-7 cells were transfected with plasmids encoding for full-length sequences of a wildtype Nrf2a, the Nrf2a^{fh318} and Nrf2a^{fh319} mutant alleles, and plasmids for Keap1a and Keap1b. A) Western blot of COS-7 cell lysates showing expression of Nrf2a proteins from the respective plasmids, transfected at 50 or 500 ng plasmid per well. Location of MW standards is shown. The predicted size of the Nrf2a protein is ~66 kDa. B) Results of transient transfection assays to evaluate the function of the Nrf2a proteins including their ability to be repressed by Keap1 and induced by the model Nrf2 activator tBHQ. Results show that the Nrf2a^{fh318} allele is capable of activating the ARE reporter at a greatly diminished capacity from the wildtype allele, but activity is above background levels. The Nrf2a^{fh319} allele has slightly less ARE activity levels than the wildtype, but is more inducible by 10 µM tBHQ. All Nrf2a proteins were repressed by Keap1a and Keap1b, except for repression of the 318-2 plasmid by Keap1b, which was not statistically significant. Two-factor ANOVA for plasmid and tBHQ exposure $p < 0.001$ followed by Fisher's PLSD. # indicates a significant difference between DMSO and tBHQ; "a" indicates a significant difference from the ARE plasmid control; "b" indicates a significant difference of the 318 or 319

plasmids from the Nrf2a wildtype plasmid activity, and “c” indicates a significant repression by Keap1 of Nrf2a-luciferase activation ($p < 0.05$). $N = 3$ replicates per group

Fig. 2. *nrf2a*^{fh318} mutant eleutheroembryos are more sensitive to PCB126 embryotoxicity and have subtle developmental abnormalities. Homozygous wildtype (WT/WT) and *nrf2a* mutant (M/M) embryos were exposed to 0, 2, or 5 nM PCB126 (with DMSO, 0.01%) at 24 hpf, and assessed for morphology at 4 days post fertilization. A) Representative eleutheroembryos from each genotype and treatment group. Quantified measures include B) ventral-dorsal length, C) swim bladder inflation, D) pericardial area, and E) severity of the craniofacial malformations. Data are from two independent experiments, which each contained 3 biological replicate pools of 5-10 embryos per dose. Statistical significance from a two-factor ANOVA and Fisher’s PLSD are designated by “#” for differences between genotypes, and “*” for PCB126 effects within a genotype; $p < 0.05$.

Fig. 3. *nrf2a*^{fh318} mutant eleutheroembryos treated with PCB126 at 5 dpf. Homozygous wildtype (WT/WT) and *nrf2a* mutant (M/M) embryos were exposed to 0, 2, or 5 nM PCB126 (with DMSO, 0.01%) at 24 hpf, and assessed for morphology at 5 days post fertilization. Quantified measures include A) ventral-dorsal distance, B) swim bladder inflation, C) pericardial area, and D) severity of the craniofacial malformations. Data are from 3-4 biological replicate pools of 5-10 embryos per dose. Statistical significance from a two-factor ANOVA and Fisher’s PLSD are designated by “#” for differences between genotypes, and “*” for PCB126 effects within a genotype; $p < 0.05$.

Fig. 4. *nrf2a*^{fh318} mutant embryos have larger yolk sacs at 3 hpf than wildtype embryos. At 3 hpf, 19-20 embryos per genotype were imaged and the yolk area was quantified. Error bar = 1000 µm. A F-test and T-test were performed in Excel using a 2-tailed distribution, and the genotypes are statistically different ($p < 0.05$).

Fig. 5. Quantitative real-time PCR measures for *ahr*-related genes in *nrf2a* wildtype and fh318 mutant eleutheroembryos at 4 dpf. Genes measured include A) *cyp1a,* B) *ahr2,* C) *ahr1a,* D) *ahr1b,* E) *ahrra,* and F) *ahrrb.* Data were analyzed by two-factor ANOVA for PCB effect, genotype effect, and interactions, followed by a one-factor ANOVA and Fisher’s PLSD ($p < 0.05$). Differences significant for PCB treatment within genotypes are noted with a “*” and differences between genotypes exposed to the same treatment are noted with a “#”. $N = 3$-4 biological replicates per group, with each replicate containing a pool of 5 fish.

Fig. 6. Quantitative real-time PCR measures for *nrf*-related genes in *nrf2a* wildtype and fh318 mutant eleutheroembryos at 4 dpf. Genes measured include A) *nrf1a,* B) *nrf1b,* C) *nrf2a,* D) *nrf3,* E) *keap1a,* and F) *keap1b.* Data were analyzed by two-factor ANOVA for PCB effect, genotype effect, and interactions, followed by a one-factor ANOVA and Fisher's PLSD ($p < 0.05$). Differences significant for PCB treatment within genotypes are noted with a "*" and differences between genotypes exposed to the same treatment are noted with a "#". *N* = 3-4 biological replicates per group, with each replicate containing a pool of 5 fish.

Fig. 7. Quantitative real-time PCR measures for *nrf2b* and regulatory targets in *nrf2a* wildtype and fh318 mutant eleutheroembryos at 4 dpf. Genes measured include A) *nrf2b,* B) *hmox1,* and C) *p53.* Data were analyzed by two-factor ANOVA for PCB effect, genotype effect, and interactions, followed by a one-factor ANOVA and Fisher's PLSD ($p < 0.05$). Differences significant for PCB treatment within genotypes are noted with a "*" and differences between genotypes exposed to the same treatment are noted with a "#". *N* = 3-4 biological replicates per group, with each replicate containing a pool of 5 fish.

Fig. 8. Quantitative real-time PCR measures for Phase II genes in *nrf2a* wildtype and fh318 mutant eleutheroembryos at 4 dpf. Genes measured include A) *nqo1* and B) *gsta1.* Data were analyzed by two-factor ANOVA for PCB effect, genotype effect, and interactions, followed by a one-factor ANOVA and Fisher's PLSD ($p < 0.05$). Differences significant for PCB treatment within genotypes are noted with a "*" and differences between genotypes exposed to the same treatment are noted with a "#". *N* = 3-4 biological replicates per group, with each replicate containing a pool of 5 fish.

Tables

Table 1. Identification of putative Antioxidant Response Elements (AREs) in the region starting 10 kb upstream from the transcription start site through the end of the 2nd exon. The zebrafish-specific (TGA(G/C)nnnTC) and mammalian (TGA(G/C)nnnGC) ARE sequences were manually identified in each genomic sequence.

Gene name	Accession #	# Zebrafish AREs	Zebrafish ARE Locations [TGA(G/C)nnnTC]	# Mammalian AREs	Mammalian ARE Locations [TGA(G/C)nnnGC]
ahr1a	NM_131028	4	-9660, -9476, -7930, -2323	5	-7774, -7691, -6079, -5434, -4814

ahr1b	NM_001024816	4	-7512, -3509, -2455, -194	3	-9819, -9262, -5418
ahr2	NM_131264	9	-8506, -8214, -6746, -2670, -74, +8889, +17669, +18540, +19184	10	-9909, -7982, -5255, -3903, -261, +7989, +8822, +11120, +12115, +15528
ahrra	NM_001035265	3	-1864, -1383, -21	4	-6279, -5659, -5036, -4907
ahrrb	NM_001033920	5	-8109, -8021, -3768, -1192, -161	1	-6395
cyp1a	NM_131879	4	-8567, -5393, +3202, +3440	4	-9968, -2472, -1965, -331
gclc	NM_199277	6	-3115, +4635, +6218, +6771, +7235, +7358	11	-9742, -6187, -5525, -4047, -3296, +178, +1741, +3460, +3772, +6043, +7223
gsta1	NM_213394	9	-9661, -5460, +3443, +4414, +4488, +4851, +9990, +11900, +15085	10	-9387, -1317, +2080, +6612, +7289, +9816, +10774, +11968, +12652, +12944
gstp1	NM_131734	4	-5560, -4371, -4061, -33	2	-5187, -1043
hmox1	NM_001127516	8	-7983, -7974, -4294, -2280, -2060, -1087, +29, +433	2	+18, +272
hsp70	NM_131397	7	-8921, -5727, -5518, -5466, -5133, -647, +218	5	-7418, -6640, -33, +1441, +1871
keap1a	NM_182864	3	-4726, -1743, +6666	8	-817, +1389, +1627, +2425, +3807, +4089, +7108, +7669
keap1b	NM_001113477	6	-9831, -6073, -5456, -3391, +536, +1234	3	-9798, -8904, -7486
nfe2l1a	NM_212855	7	-7436, -6034, -5484, -1461, +3531, +8657, +9025	3	-6657, +1805, +9766
nfe2l1b	NM_001278842	10	-8942, -7257, -6739, -5758, -5670, -1929, -748, -31, +1859, +3480	4	-3736, -2234, +1803, +2683
nfe2l2a	NM_182889	4	-5710, -5431, -5355, +3418	3	-2812, +1685, +13484
nfe2l2b	NM_001257183	5	-9572, -1293, -1116, +2636, +3853	5	-6837, -4311, +2366, +4102, +5007
nfe2l3	NM_213231	2	-5360, -3675	6	-9497, -9121, -7259, -6205, +857, +1437
nqo1	NM_001204272	0		3	-9195, -5399, +3781

1085

Table 2. Comparison of changes in gene expression between Nrf2a wildtype (wt) and Nrf2afh318/fh318 (m) embryos at 96 hpf. Expression levels that were not different between wt and m are indicated with "=" while < and > indicate that the wt fish had expression either significantly less than or greater than the mutants.

Gene names	**Basal expression**	**PCB126 inducible**
ahr2	wt = m	wt = m
cyp1a	wt = m	wt < m
ahrra, ahrrb, nrf2a	wt = m	wt > m
ahr1a, hmox1, keap1a, keap1b, nrf1a, nrf2b, nrf3	wt = m	wt
ahr1b	wt > m	wt
nrf2b	wt = m	m
gclc, gstp1, hsp70, nfe2, tp53	wt = m	-
gsta1, nqo1	wt < m	-

Figures

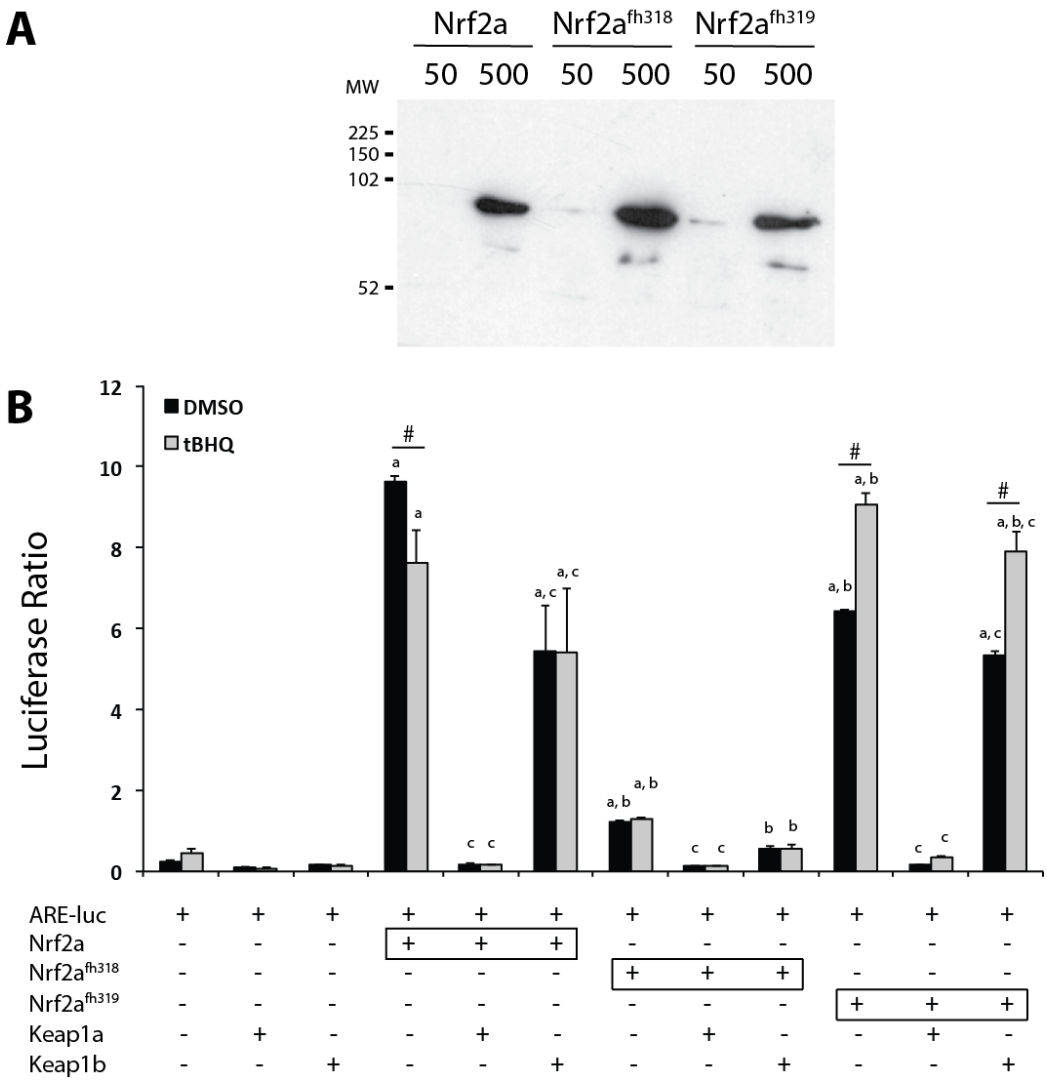

Fig. 1. Activation of ARE-driven luciferase reporter by Nrf2a mutant alleles *in vitro.* COS-7 cells were transfected with plasmids encoding for full-length sequences of a wildtype Nrf2a, the Nrf2a^{fh318} and Nrf2a^{fh319} mutant alleles, and plasmids for Keap1a and Keap1b. A) Western blot of COS-7 cell lysates showing expression of Nrf2a proteins from the respective plasmids, transfected at 50 or 500 ng plasmid per well. Location of MW standards is shown. The predicted size of the Nrf2a protein is ~66 kDa. B) Results of transient transfection assays to evaluate the function of the Nrf2a proteins including their ability to be repressed by Keap1 and induced by the model Nrf2 activator tBHQ. Results show that the Nrf2a^{fh318} allele is capable of activating the ARE reporter at a greatly diminished capacity from the wildtype allele, but activity is above background levels. The Nrf2a^{fh319} allele has slightly less ARE activity levels than the wildtype, but is more inducible by 10 µM tBHQ. All Nrf2a proteins were repressed by Keap1a and Keap1b, except for repression of the 318-2 plasmid by Keap1b, which was not statistically

significant. Two-factor ANOVA for plasmid and tBHQ exposure $p < 0.001$ followed by Fisher's PLSD. # indicates a significant difference between DMSO and tBHQ; "a" indicates a significant difference from the ARE plasmid control; "b" indicates a significant difference of the 318 or 319 plasmids from the Nrf2a wildtype plasmid activity, and "c" indicates a significant repression by Keap1 of Nrf2a-luciferase activation ($p < 0.05$). $N = 3$ replicates per group.

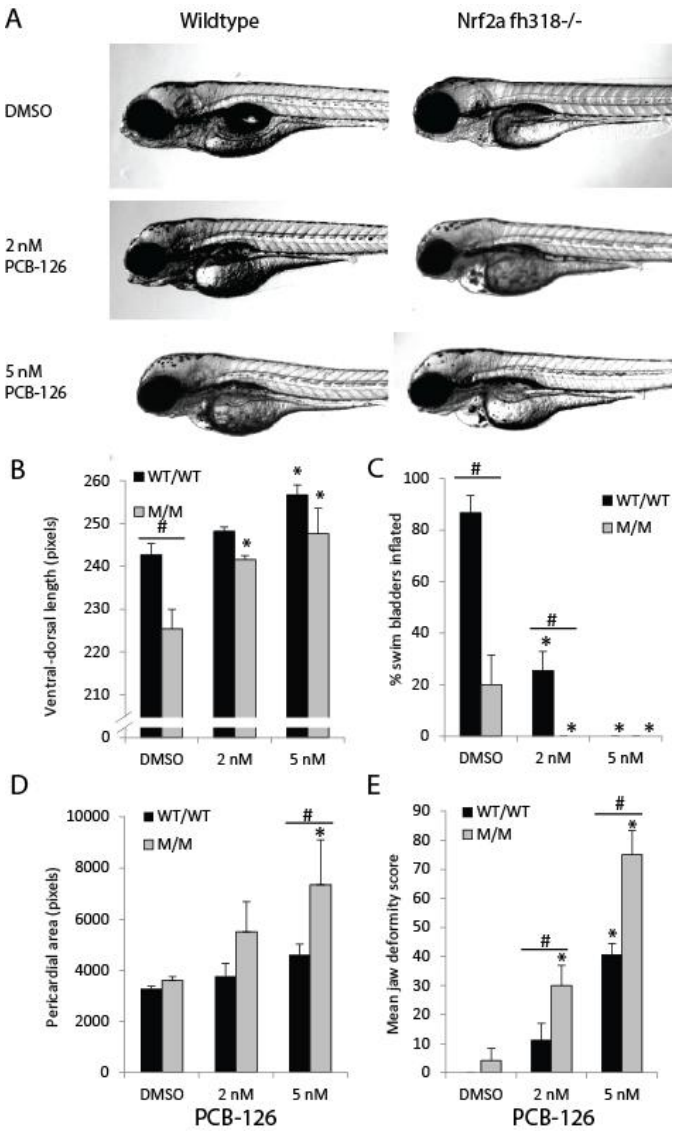

Fig. 2. *nrf2a*^{fh318} mutant eleutheroembryos are more sensitive to PCB126 embryotoxicity and have subtle developmental abnormalities. Homozygous wildtype (WT/WT) and *nrf2a* mutant (M/M) embryos were exposed to 0, 2, or 5 nM PCB126 at 24 hpf, and assessed for morphology at 4 days post fertilization. A) Representative eleutheroembryos from each genotype and treatment group. Quantified measures include B) ventral-dorsal length, C) swim bladder inflation, D) pericardial area, and E) severity of the craniofacial malformations. Data are from two independent experiments, which each contained 3 biological replicate pools of 5-10 embryos per dose. Statistical significance from a two-factor ANOVA and Fisher's PLSD are designated by "#" for differences between genotypes, and "*" for PCB126 effects within a genotype; $p < 0.05$.

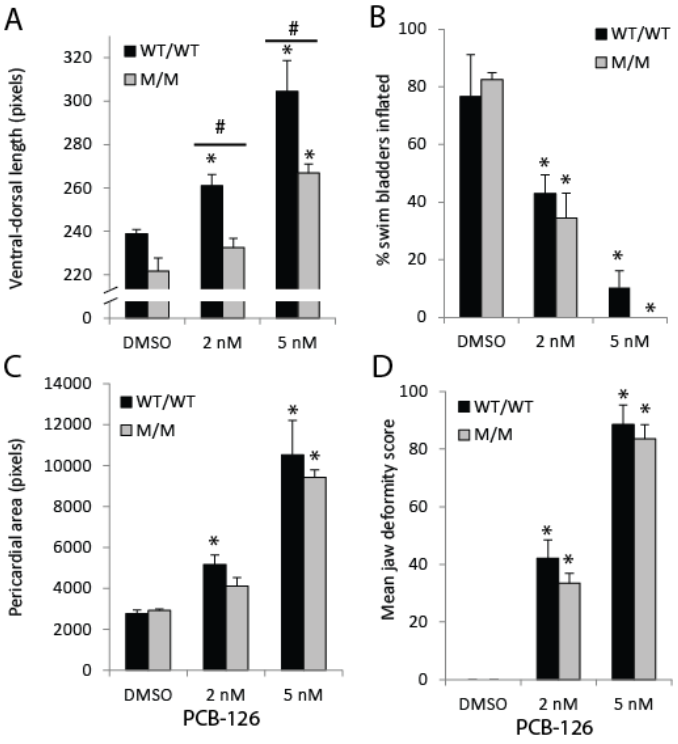

Fig. 3. *nrf2a*^{fh318} mutant eleutheroembryos treated with PCB126 at 5 dpf. Homozygous wildtype (WT/WT) and *nrf2a* mutant (M/M) embryos were exposed to 0, 2, or 5 nM PCB126 at 24 hpf, and assessed for morphology at 5 days post fertilization. Quantified measures include A) ventral-dorsal distance, B) swim bladder inflation, C) pericardial area, and D) severity of the craniofacial malformations. Data are from 3-4 biological replicate pools of 5-10 embryos per dose. Statistical significance from a two-factor ANOVA and Fisher's PLSD are designated by "#" for differences between genotypes, and "*" for PCB126 effects within a genotype; $p < 0.05$.

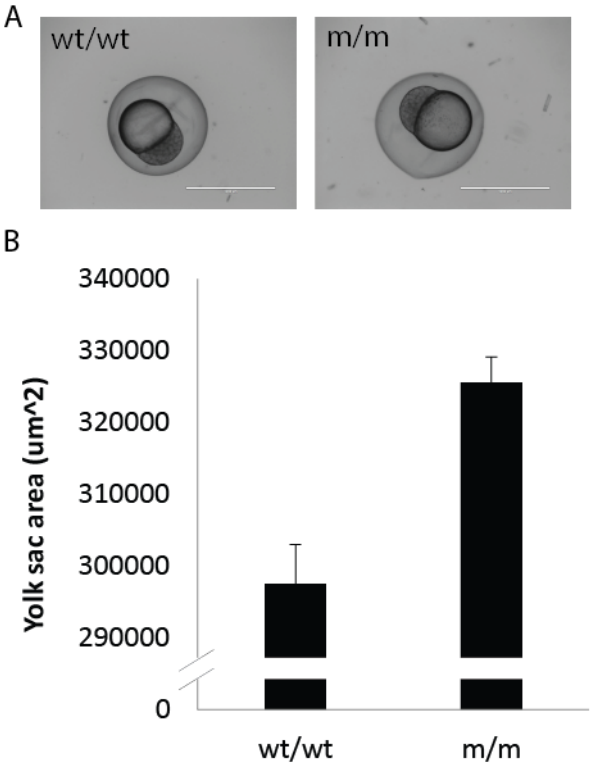

Fig. 4. *nrf2a* mutant embryos have larger yolk sacs at 3 hpf than wildtype embryos. At 3 hpf, 19-20 embryos per genotype were imaged and the yolk area was quantified. A) Representative embryos from the wildtype and fh318 mutants; error bar = 1000 µm. B) Quantification of the yolk sacs. A F-test and T-test were performed in Excel using a 2-tailed distribution, and the genotypes are statistically different ($p < 0.05$).

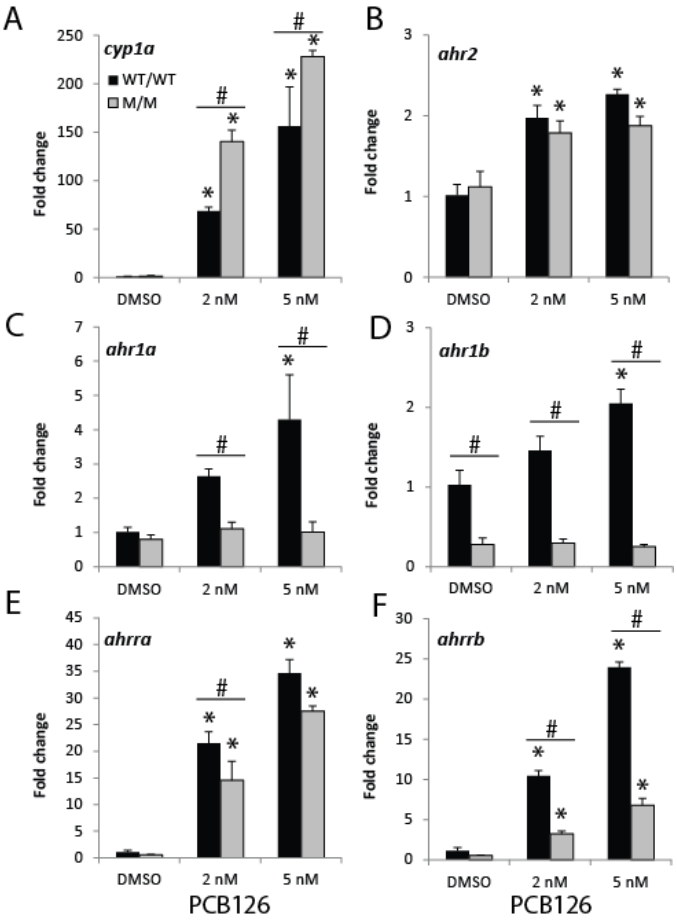

Fig. 5. Quantitative real-time PCR measures for *ahr*-related genes in *nrf2a* wildtype and mutant eleutheroembryos at 4 dpf. Genes measured include A) *cyp1a,* B) *ahr2,* C) *ahr1a,* D) *ahr1b,* E) *ahrra,* and F) *ahrrb.* Data were analyzed by two-factor ANOVA for PCB effect, genotype effect, and interactions, followed by a one-factor ANOVA and Fisher's PLSD ($p < 0.05$). Differences significant for PCB treatment within genotypes are noted with a "*" and differences between genotypes exposed to the same treatment are noted with a "#". N = 3-4 biological replicates per group, with each replicate containing a pool of 5 fish.

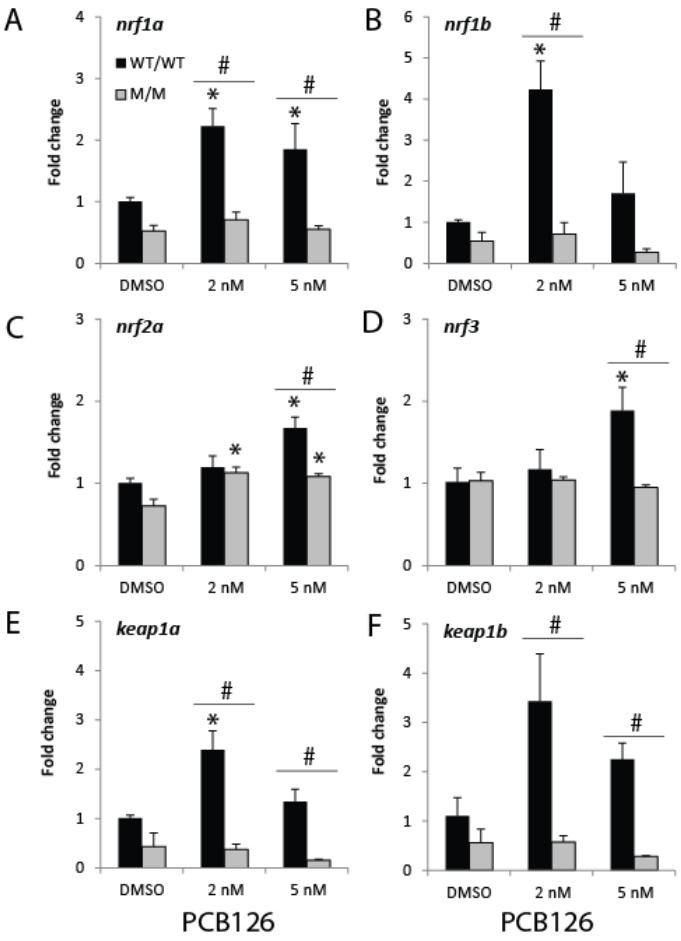

1153

1154 Fig. 6. Quantitative real-time PCR measures for *nrf*-related genes in *nrf2a* wildtype and mutant
1155 eleutheroembryos at 4 dpf. Genes measured include A) *nrf1a,* B) *nrf1b,* C) *nrf2a,* D) *nrf3,* E)
1156 *keap1a,* and F) *keap1b.* Data were analyzed by two-factor ANOVA for PCB effect, genotype
1157 effect, and interactions, followed by a one-factor ANOVA and Fisher's PLSD ($p < 0.05$).
1158 Differences significant for PCB treatment within genotypes are noted with a "*" and differences
1159 between genotypes exposed to the same treatment are noted with a "#". N = 3-4 biological
1160 replicates per group, with each replicate containing a pool of 5 fish.

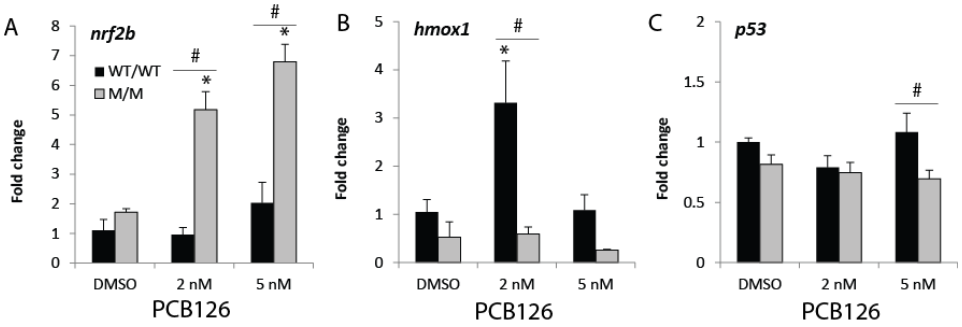

Fig. 7. Quantitative real-time PCR measures for *nrf2b* and regulatory targets in *nrf2a* wildtype and mutant eleutheroembryos at 4 dpf. Genes measured include A) *nrf2b,* B) *hmox1,* and C) *p53.* Data were analyzed by two-factor ANOVA for PCB effect, genotype effect, and interactions, followed by a one-factor ANOVA and Fisher's PLSD ($p < 0.05$). Differences significant for PCB treatment within genotypes are noted with a "*" and differences between genotypes exposed to the same treatment are noted with a "#". *N* = 3-4 biological replicates per group, with each replicate containing a pool of 5 fish.

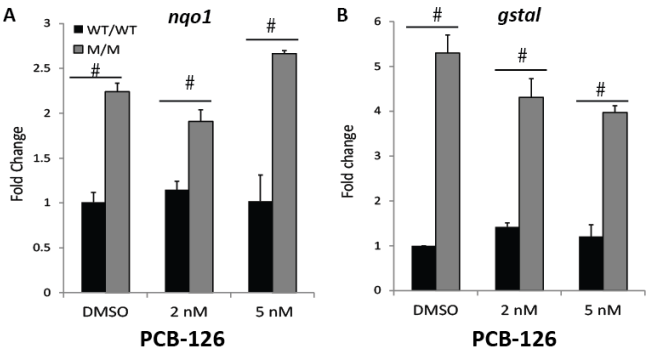

1170

1171 Fig. 8. Quantitative real-time PCR measures for Phase II genes in *nrf2a* wildtype and mutant
1172 eleutheroembryos at 4 dpf. Genes measured include A) *nqo1* and B) *gsta1.* Data were analyzed
1173 by two-factor ANOVA for PCB effect, genotype effect, and interactions, followed by a one-factor
1174 ANOVA and Fisher's PLSD ($p < 0.05$). Differences significant for PCB treatment within
1175 genotypes are noted with a "*" and differences between genotypes exposed to the same
1176 treatment are noted with a "#". *N* = 3-4 biological replicates per group, with each replicate
1177 containing a pool of 5 fish.

1178 Supplemental Table 1. List of qPCR primers, melting temperature, and sources.

Gene	Forward primer (5'-3') Reverse primer (5'-3')	Tm	Reference
ahr1a	TTGTTCTTGGCTACACAGAGGCAGAGC CCCAGTTTCACCGGTCCTCATCATCC	66	Karchner *et al.,* 2005
ahr1b	GGTTTGTCGTCAAACAACAGTAACCACG CCACCAACACAAAGCCATTAAGAGCCTG	65	Karchner *et al.,* 2005
ahr2	CTACTTGGGCTTCCATCAGTCG GTCACTTGAGGGATTGAGAGCG	65	Evans *et al.,* 2005
ahrra	GCGCATCAAGAGCTTCTGCAGCGTGTT CCACTGACGACCAGCGCAAACCCT	65	Evans *et al.,* 2005
ahrrb	AAACAGAAGCTCTGGCCGCAGTGA CTGTATGCCCATGAAGCGTCCTGAG	65	Evans *et al.,* 2005
b-actin	CAACAGAGAGAAGATGACACAGATCA GTCACACCATCACCAGAGTCCATCAC	65	Evans *et al.,* 2005
cyp1a	GCATTACGATACGTTCGATAAGGAC GCTCCGAATAGGTCATTGACGAT	65	Evans *et al.,* 2005
ef1a	CTTCTCAGGCTGACTGTGC CCGCTAGGATTACCCTCC	60	McCurley & Callard, 2008
gclc	AACCGACACCCAAGATTCAGCACT CCATCATCCTCTGGAAACACCTCC	60	Timme-Laragy *et al.,* 2009
gsta1	TCACACCTGCCGAAAACAAAG CCACGAGGAAAGAAGAGTTTGC	65	Richter *et al.,* 2011
gstp1	CGACTTGAAAGCCACCTGTGTC CTGTCGTTTTTGCCATATGCAGC	67	Timme-Laragy *et al*., 2012
hmox1	GCTTCTGCTGTGCTCTCTATACG CCAATCTCTCTCAGTCTCTGTGC	62	Timme-Laragy *et al*., 2012
hsp70	CAAAGGCAAATCCTCAGAGC CACAAAGTGGTTCACCATGC	64	Timme-Laragy *et al*., 2012
keap1a	CCGGTTGTCCCCGTCAAACC CCGGTTGTCCCCGTCAAACC	65	-
keap1b	CCAGATCGACAGCGTGGTTC CCTGGCTGAAGTTCATGTAG	65	-
nfe2	AATTTGGAGATGGACTTGGCCTGG GCATCACAAGTGGCTGGAATGGAT	60	Timme-Laragy *et al*., 2012
nqo1	TTCAGTACCCACTCTACTGG GCATGGCCCTCTTATTCTTG	63	Hahn *et al.,* 2014

nrf1a	CCAGAGTTGACAGGTCCTGG CATAACCTGTGATTCCATGATAGAC	64	Timme-Laragy *et al*., 2012
nrf1b	GCAGGACATGGAGGTGAACAATACG GGATCGTGGGAGCCCAAAATTTCC	66	Timme-Laragy *et al*., 2012
nrf2a	GAGCGGGAGAAATCACACAGAATG CAGGAGCTGCATGCACTCATCG	65	Timme-Laragy *et al*., 2012
nrf2b	GGCAGAGGGAGGAGGAGACCAT AAACAGCAGGGCAGACAACAAGG	68	Timme-Laragy *et al*., 2012
nrf3	GCATGAGGATTTAGTGGTTAGTGG GGAGTCAAAATCATCAAAGTCAG	64	Timme-Laragy *et al*., 2012
tp53	CCCGGATGGAGATAACTTG CACAGTTGTCCATTCAGCAC	60	Duan *et al.,* 2011

1179

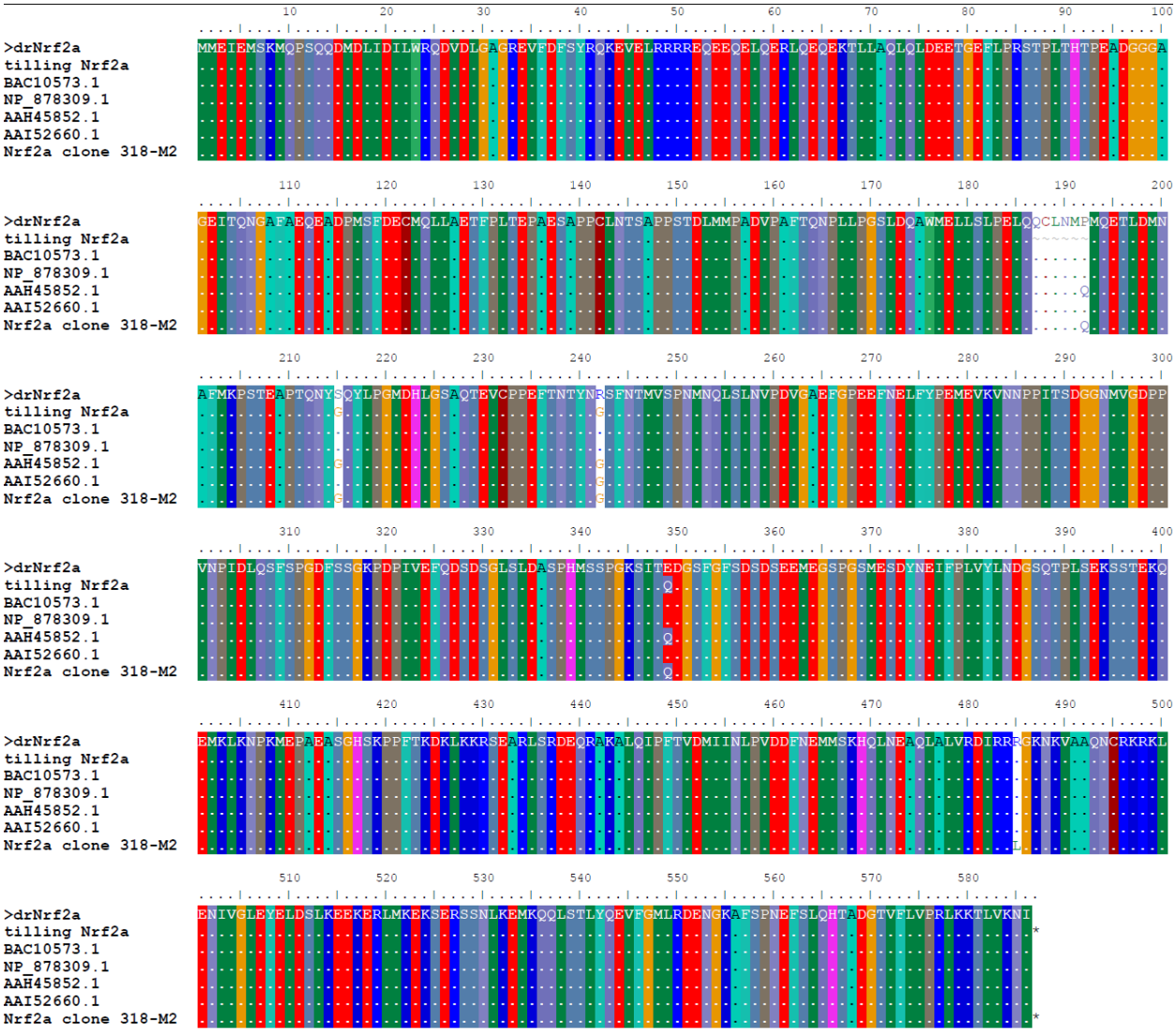

Supplemental Figure 1. Protein alignment of the translated *nrf2a*^{fh318} allele with other Nrf2a protein sequences.

Source of sequences: drNrf2a (consensus sequence); "tilling Nrf2a" (http://research.fhcrc.org/moens/en/mutants.html); BAC10573.1 (Kobayashi et al 2002); NP_878309.1 (GenBank reference sequence, derived from BAC10573.1); AAH45852.1 (GenBank direct submission); AAI52660.1 (GenBank direct submission); Nrf2a clone 318-M2 (our sequence of mutant fh318).

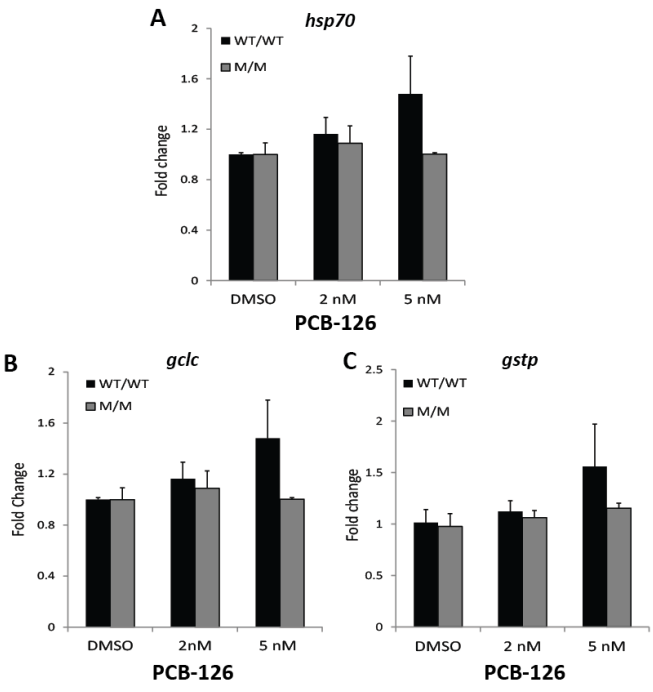

1188

1189 Supplemental Fig. 2. . Quantitative real-time PCR measures for oxidative stress response
1190 genes in *nrf2a* wildtype and fh318 mutant eleutheroembryos at 4 dpf. Genes measured include
1191 A) *hsp70,* B) *gclc,* and C) *gstp1.* Data were analyzed by two-factor ANOVA for PCB effect,
1192 genotype effect, and interactions, followed by a one-factor ANOVA and Fisher's PLSD ($p <$
1193 0.05). N = 3-4 biological replicates per group, with each replicate containing a pool of 5 fish.

1194

Supplemental References:

Duan, J., Ba, Q., Wang, Z., Hao, M., Li, X., Hu, P., Zhang, D., Zhang, R., and Wang, H. (2011). Knockdown of ribosomal protein S7 causes developmental abnormalities via p53 dependent and independent pathways in zebrafish. Int J Biochem Cell Biol 43(8), 1218-27, 10.1016/j.biocel.2011.04.015.

Evans, B. R., Karchner, S. I., Franks, D. G., and Hahn, M. E. (2005). Duplicate aryl hydrocarbon receptor repressor genes (ahrr1 and ahrr2) in the zebrafish Danio rerio: structure, function, evolution, and AHR-dependent regulation in vivo. Archives of biochemistry and biophysics 441(2), 151-67, 10.1016/j.abb.2005.07.008.

Hahn, M. E., McArthur, A. G., Karchner, S. I., Franks, D. G., Jenny, M. J., Timme-Laragy, A. R., Stegeman, J. J., Woodin, B. R., Cipriano, M. J., and Linney, E. (2014). The transcriptional response to oxidative stress during vertebrate development: effects of tert-butylhydroquinone and 2,3,7,8-tetrachlorodibenzo-p-dioxin. PloS one 9(11), e113158, 10.1371/journal.pone.0113158.

Karchner, S. I., Franks, D. G., and Hahn, M. E. (2005). AHR1B, a new functional aryl hydrocarbon receptor in zebrafish: tandem arrangement of ahr1b and ahr2 genes. The Biochemical journal 392(Pt 1), 153-61, 10.1042/bj20050713.

Kobayashi, M., Itoh, K., Suzuki, T., Osanai, H., Nishikawa, K., Katoh, Y., Takagi, Y., and Yamamoto, M. (2002). Identification of the interactive interface and phylogenic conservation of the Nrf2-Keap1 system. *Genes to cells : devoted to molecular & cellular mechanisms* **7**(8), 807-20.

McCurley, A. T., and Callard, G. V. (2008). Characterization of housekeeping genes in zebrafish: male-female differences and effects of tissue type, developmental stage and chemical treatment. BMC Mol Biol 9, 102, 10.1186/1471-2199-9-102.

Richter, C. A., Garcia-Reyero, N., Martyniuk, C., Knoebl, I., Pope, M., Wright-Osment, M. K., Denslow, N. D., and Tillitt, D. E. (2011). Gene expression changes in female zebrafish (Danio rerio) brain in response to acute exposure to methylmercury. Environmental toxicology and chemistry / SETAC 30(2), 301-8, 10.1002/etc.409.

Timme-Laragy, A. R., Karchner, S. I., Franks, D. G., Jenny, M. J., Harbeitner, R. C., Goldstone, J. V., McArthur, A. G., and Hahn, M. E. (2012). Nrf2b, novel zebrafish paralog of oxidant-responsive transcription factor NF-E2-related factor 2 (NRF2). The Journal of biological chemistry 287(7), 4609-27, 10.1074/jbc.M111.260125.

Timme-Laragy, A. R., Van Tiem, L. A., Linney, E. A., and Di Giulio, R. T. (2009). Antioxidant responses and NRF2 in synergistic developmental toxicity of PAHs in zebrafish. Toxicological sciences : an official journal of the Society of Toxicology 109(2), 217-27, 10.1093/toxsci/kfp038.